




Geochemistry, Geophysics, Geosystems®



RESEARCH ARTICLE

10.1029/2023GC011295

Halogen (F, Cl, Br, and I) Devolatilization During Prograde Subduction: Insights From Western Alps Ophiolites

G. M. Beaudoin¹, J. D. Barnes¹ , O. F. Orlandini¹, R. Chatterjee¹, D. F. Stockli¹ , and T. John² 

¹Department of Geological Sciences, University of Texas, Austin, TX, USA, ²Institut für Geologische Wissenschaften, Freie Universität Berlin, Berlin, Germany

Key Points:

- Exhumed ophiolites in the Western Alps record prograde subduction zone metamorphism and halogen devolatilization of altered ocean crust
- Results show halogen decoupling. Fluorine is retained, whereas heavy halogens are mobilized from mafic rocks in the subducting slab
- Devolatilization of altered ocean crust occurs early in subduction; a significant portion of Cl, Br, and I is lost prior to eclogite facies

Supporting Information:

Supporting Information may be found in the online version of this article.

Correspondence to:

J. D. Barnes,
jdbarnes@jsg.utexas.edu

Citation:

Beaudoin, G. M., Barnes, J. D., Orlandini, O. F., Chatterjee, R., Stockli, D. F., & John, T. (2024). Halogen (F, Cl, Br, and I) devolatilization during prograde subduction: Insights from Western Alps ophiolites. *Geochemistry, Geophysics, Geosystems*, 25, e2023GC011295. <https://doi.org/10.1029/2023GC011295>

Received 12 OCT 2023

Accepted 1 MAR 2024

Author Contributions:

Conceptualization: G. M. Beaudoin,

J. D. Barnes, T. John

Data curation: G. M. Beaudoin

Formal analysis: G. M. Beaudoin,

O. F. Orlandini, R. Chatterjee

Funding acquisition: J. D. Barnes

Investigation: G. M. Beaudoin,

J. D. Barnes, T. John

Methodology: G. M. Beaudoin,

J. D. Barnes, O. F. Orlandini,

R. Chatterjee, D. F. Stockli

© 2024 The Authors. *Geochemistry, Geophysics, Geosystems* published by Wiley Periodicals LLC on behalf of American Geophysical Union.

This is an open access article under the terms of the [Creative Commons Attribution-NonCommercial-NoDerivs License](https://creativecommons.org/licenses/by/4.0/), which permits use and distribution in any medium, provided the original work is properly cited, the use is non-commercial and no modifications or adaptations are made.

Abstract In order to examine the progressive chemical evolution of halogens (F, Cl, Br, I) in altered ocean crust (AOC) during prograde subduction, this study compares bulk and in situ halogen concentrations in mafic samples from three petrogenetically related exhumed terrains in the Western Alps (the Chenaillet ophiolite, the Queyras ophiolites of the Schistes Lustrés, and the Monviso ophiolite). Samples from the Chenaillet ophiolite represent oceanic crust unaffected by metamorphic halogen loss and define a protolith halogen content (122 $\mu\text{g/g}$ F, 29 $\mu\text{g/g}$ Cl, 82 ng/g Br, and 98 ng/g I). Samples from the Queyras ophiolites experienced blueschist facies conditions, undergoing recrystallization and halogen loss (74 $\mu\text{g/g}$ F, 19 $\mu\text{g/g}$ Cl, 70 ng/g Br, and 63 ng/g I). Eclogite facies samples from the Monviso meta-ophiolite exhibit markedly reduced Cl (8 $\mu\text{g/g}$ Cl) and Br (42 ng/g Br) contents relative to samples from Chenaillet and Queyras. Using electron probe microanalysis (EPMA), F and Cl host minerals (e.g., amphibole, chlorite, epidote) are identified and characterized in selected samples, showing a broad distribution of F and Cl, lending support to the view that halogen devolatilization in the subducting slab occurs continuously and is not dependent on the breakdown of a particular phase. In situ Cl concentrations decrease significantly between sub-greenschist and blueschist assemblages. Fluorine is retained within subducting AOC and is decoupled from the heavy halogens (Cl, Br, I), which undergo continuous devolatilization during prograde metamorphism.

Plain Language Summary Halogens are volatile elements found predominantly in the Earth's oceans and sediments. During hydrothermal processes, they bond with other elements to form volatile-bearing minerals. Tectonic processes can bring halogen-enriched rocks into subduction zones, regions where one tectonic plate submerges beneath another. Subduction governs the transport of material from Earth's surface to its interior, influencing the chemical evolution of the crust, atmosphere, hydrosphere, and mantle. As the subducting plate carries rocks to greater depths beneath the surface, volatile-bearing minerals destabilize, releasing volatile components as fluids. Halogens alter the properties of subduction-derived fluids and impact the behavior of other biologically, climatically, and economically important elements (e.g., H_2O , CO_2 , Au). Due to the influential role of halogens in subduction zone environments, the timing and extent of halogen loss must be constrained. This study investigates metamorphic rock samples from the Western Alps which underwent halogen-enrichment followed by subduction and devolatilization. Results show that halogens behave differently from each other. Fluorine is not removed; it is retained until deep in the subduction zone and is returned to the Earth's mantle. The efficient removal of the other halogens occurs early in subduction (<60 km depth) and is not linked to the destabilization of a specific mineral.

1. Introduction

As elements with moderately to strongly incompatible and volatile behaviors during volcanic and magmatic processes, halogens (F, Cl, Br, and I) are enriched in Earth's surface reservoirs. They are primarily enriched in seawater and sediments, and depleted in the mantle. Despite low mantle abundances (e.g., Kendrick et al., 2017), halogens are observed in mantle-derived samples, including ocean island basalts (OIB) (e.g., Hauri, 2002; Kendrick, Jackson, et al., 2015; Stroncik & Haase, 2004), back-arc basin basalts (BABB) (e.g., Kendrick, Arculus, et al., 2014; Kendrick, Danyushevsky, et al., 2020; Kent et al., 2002; Sun et al., 2007), and as common volatile emissions from subaerial volcanoes (e.g., Aiuppa et al., 2009). These halogen-rich mantle-derived products point to the addition of halogens to the mantle from the recycling of surface reservoirs. Subduction zones represent locations of geochemical cycling between Earth's surface and its interior and serve as the mechanism by which halogens are reintroduced to the mantle.

Resources: J. D. Barnes, D. F. Stockli
Supervision: J. D. Barnes
Validation: G. M. Beaudoin, J. D. Barnes
Visualization: G. M. Beaudoin
Writing – original draft: G. M. Beaudoin
Writing – review & editing: J. D. Barnes, D. F. Stockli, T. John

During subduction, the progressive breakdown of hydrous mineral phases releases aqueous fluids back into the mantle. Due to their hydrophilic nature, heavy halogens (Cl, Br, and I) are expected to partition strongly into the fluid phase (e.g., Manning, 2004), stripping the down-going slab of halogens prior to reaching depths of arc magma genesis and returning those elements to the surface. However, current models of global halogen cycling propose estimates for trench inputs that are greater than arc outputs (e.g., Barnes et al., 2018), likely due to unresolved halogen outfluxes through the forearc and to the mantle. To refine geochemical cycles, more work is needed to constrain the behavior of halogens during metamorphism, particularly within altered oceanic crust (AOC).

Due to its large volume compared to subducting sediments and protracted interactions with seawater and marine sediments, oceanic crust represents a significant halogen reservoir. During hydrothermal alteration, basalts and gabbros form secondary alteration phases that can host halogens. Due to the large ionic sizes of Br and I and the redox sensitivity of I, structural incorporation is less favorable than for F and Cl, which substitute for OH⁻ in hydrous minerals (e.g., Volfanger et al., 1985). Potential Br- and I-bearing phases may include phyllosilicates, amphiboles, carbonates, and Fe-oxyhydroxides (Chavrit et al., 2016; Kendrick, 2019b; Kendrick, Caulfield, et al., 2020). Additionally, halogens may be hosted within fluid inclusions, crystal defects, and along grain boundaries. A number of studies have measured the halogen content in drill core samples of AOC from the seafloor (Beaudoin et al., 2022; Chavrit et al., 2016; Kendrick, 2019a, 2019b). However, only three studies have measured the full suite of halogens (F, Cl, Br, and I) in subducted AOC (Beaudoin et al., 2022; Hughes et al., 2018; Pagé et al., 2016), and none have systematically investigated the halogen budget within a related suite of samples from different metamorphic grades, a goal of this study.

Mafic samples ($n = 14$) from five ophiolites from the Western Alps were selected for this work. These ophiolites experienced a range of peak P - T conditions, from sub-greenschist to eclogite facies and record prograde changes in the halogen content of subducting ocean crust. In this study, bulk and in situ halogen concentrations are determined in order to (a) characterize the content of structurally bound halogens in basaltic and gabbroic rock samples from three metamorphic grades: sub-greenschist facies, blueschist facies, and eclogite facies; (b) quantify changes to the halogen budget resulting from progressive metamorphism and devolatilization; (c) relate those changes to mineralogical controls; and (d) establish whether Alpine subduction zone metamorphism—and the ophiolites which resulted from it—are representative and should be used to inform the understanding of halogen cycling in other subduction systems.

2. Geologic Setting and Sample Descriptions

The Alpine orogenic chain marks the early Cenozoic collision of the Eurasian plate with northern Africa after a cycle of rifting and subduction (e.g., Agard, 2021; Schmid et al., 1996). Exhumed continental and oceanic units experienced metamorphic conditions ranging from greenschist facies to ultrahigh-pressure (UHP) eclogite facies conditions (e.g., Chopin, 1984; Goffé et al., 2004). This study will focus on the western arc of the Liguro-Piemont Zone, which preserves ophiolites and marine sedimentary rocks from the subducted Alpine Tethys Ocean. Subduction began 110–80 Ma and proceeded with a metamorphic geothermal gradient of 7–8°C/km (Agard, 2021; Agard et al., 2001).

There is a debate regarding the nature and maturity of the Alpine Tethys Ocean crust. Geochemical signatures support a mantle source of N-MORB type composition (Chalot-Prat et al., 2003). However, the ophiolites of the Western Alps lack conventional Penrose style stratigraphy (e.g., Tricart & Lemoine, 1991). Alpine ophiolites are typically consistent with formation in slow- to ultraslow-spreading, magma-poor ridge environments that may represent an ocean-continent transition zone rather than a true ocean basin (Manatschal & Müntener, 2009). Li et al. (2013) estimate spreading rates of 3 cm/yr for the Alpine Tethys Ocean. In order to examine progressive metamorphism, three localities within the Western Alps have been selected, from low- to high-metamorphic grade they are: the Chenaillet ophiolite, ophiolites within the Queyras region, and the Monviso ophiolite. Figure 1 shows sampling locations, the locations of mafic and ultramafic ophiolites, and the west-to-east increase in peak metamorphic conditions experienced by rocks in the Queyras region of the Schistes Lustrés complex.

2.1. Chenaillet Ophiolite

Located in south-eastern France, the Chenaillet ophiolite is a structural klippe (Figure 1b) interpreted as a section of obducted ocean crust (e.g., Li et al., 2013; Manatschal et al., 2011; Mével et al., 1978). The ophiolite

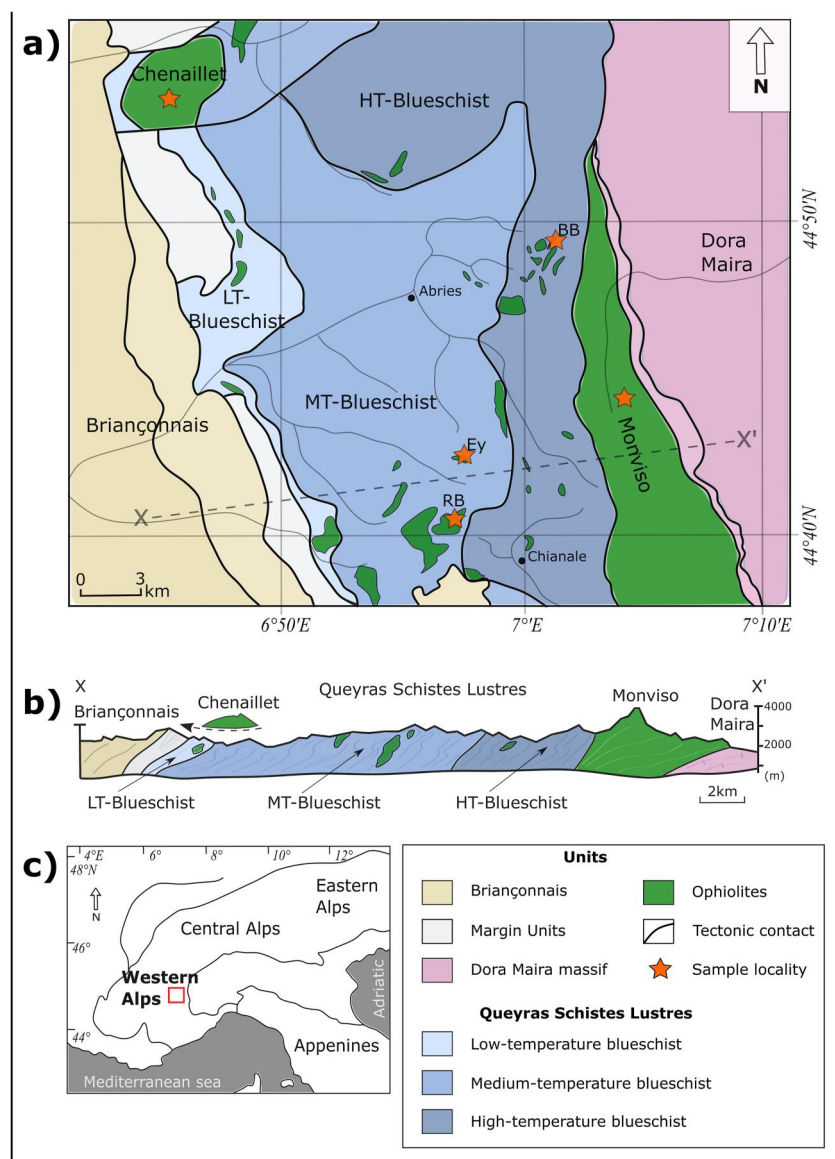


Figure 1. Map of the Western Alps showing metamorphic grade and locations of ophiolites. (a) Simplified geologic map of the study area with major tectonic contacts and units. The metamorphic grade increases from west to east. Sampling locations are marked by orange stars. BB = Bric Bouchet, Ey = Crête de l'Eychassier, RB = Rocca Bianca. (b) Cross-section through the study area. Trace of cross-section, XX', shown as dashed line in (a). (c) Tectonic sketch of Western Europe, study region shown in red. Figure modified from Lafay et al. (2013) and Schwartz et al. (2013).

experienced hydrothermal seafloor alteration after crystallization at approximately 165 Ma (Li et al., 2013). Chenaillet escaped subduction and bears a minor sub-greenschist facies overprint from collisional deformation ($T < 300^{\circ}\text{C}$, $P < 0.4$ GPa; Figure 2; Schwartz et al., 2013). Chenaillet is composed of basal serpentinite, discontinuous gabbro bodies, a thick volcanic section (basaltic flows and pillows), and rare sedimentary intercalations (Manatschal et al., 2011). Like previous authors (e.g., Debret et al., 2016; Lafay et al., 2013; Philippot et al., 1998), this study uses Chenaillet to represent the protolith of subducted oceanic crust in the Alps.

Four samples were selected from Chenaillet. Samples include two gabbros and two basalts. Sample H17-B814A02 is a coarse-grained Mg-gabbro sampled from the middle of the stratigraphic section. In the upper section, another gabbroic sample, H17-B815B02, was collected from the top of the Mg-gabbro unit just below the contact with basalt. Samples H17-B815C03-I and H17-B815C03-C are basaltic samples collected from the

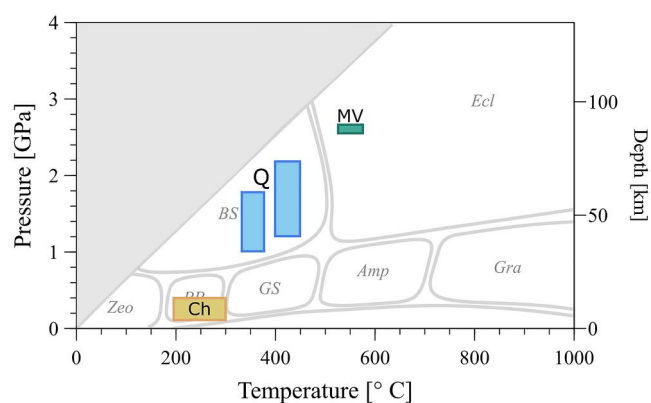


Figure 2. Pressure-Temperature plot showing estimates of peak metamorphic conditions for sample localities considered in this study (see text for details and references). Fields outlined in gray represent metamorphic facies. Ch = Chenaillet, Q = Queyras, MV = Monviso.

mantle and core, respectively, of a large basalt pillow near the bottom of the stratigraphic section. Sample description, mineralogy, and location are summarized in Table 1.

2.2. Queyras Ophiolites

Southeast of the Chenaillet ophiolite is the Queyras region (Figure 1a), an area characterized by a thick sequence of the heterogeneous Schistes Lustrés, a regionally extensive belt of calcschists, shales, and limestones deposited in the Tethyan ocean and metamorphosed to blueschist conditions in the accretionary prism (e.g., Agard, 2021; Agard et al., 2001; Herviou et al., 2022). Though previously interpreted as a mélange, detailed mapping has revealed ophiolite sequences of associated serpentinite, gabbro, basalt, and sedimentary rocks previously masked by complex large-scale folding (Tricart & Schwartz, 2006). Samples were collected from three ophiolite slivers within the Queyras region: Rocca Bianca, Crête de l'Eychassier, and Bric Bouchet. These slivers in the Queyras region share features with ocean crust formed in slow-spreading centers, similar to those in the Northern

Atlantic, which produce thin basaltic sections, no sheeted dike complexes, and discontinuous gabbroic bodies in association with serpentinitized peridotites. Crête de l'Eychassier is characterized by pelagic sedimentary, gabbroic, and ultramafic rocks that experienced peak metamorphic conditions of $\sim 340\text{--}370^\circ\text{C}$ and $\sim 1.0\text{--}1.7$ GPa (Herviou et al., 2022; Schwartz et al., 2013). Rocca Bianca is composed of pelagic sedimentary, basaltic, gabbroic, and ultramafic rocks that reached $\sim 360^\circ\text{C}$ and $\sim 1.0\text{--}1.7$ GPa (Herviou et al., 2022; Schwartz et al., 2013). Bric Bouchet exposes sedimentary rocks and basalts (Tricart & Lemoine, 1991) that experienced higher metamorphic temperatures and pressures ($\sim 400\text{--}450^\circ\text{C}$ and $\sim 1.2\text{--}2.1$ GPa; Herviou et al., 2022; Schwartz et al., 2013). A summary of metamorphic conditions is depicted in Figure 2.

Four samples (Table 1) were selected from the Queyras Valley; samples come from three ophiolites that experienced blueschist facies conditions. The peak metamorphic pressure and temperature gradient increases from west to east within the Queyras Valley; one sample from Crête de l'Eychassier and two samples from Rocca Bianca represent mafic rocks subducted to medium-temperature blueschist conditions, and one sample from Bric Bouchet represents mafic rocks subducted to high-temperature blueschist conditions. All analyzed samples collected from the Queyras Valley are thought to have gabbroic protoliths. Due to complex field relations, poor exposures, and pervasive metasomatic overprinting, the metabasalts collected from the Queyras region were ultimately determined to be unsuitable for this study. Queyras metagabbro samples display partial equilibration to blueschist facies conditions, as demonstrated by the preservation of magmatic cores of pyroxene. Partial equilibration could suggest limited hydration of these samples at the seafloor prior to subduction, thereby inhibiting the formation of pervasive blueschist-facies hydrous phases.

2.3. Monviso Ophiolite

East of Queyras (Figure 1a), the Monviso meta-ophiolite in northwest Italy extends for more than 30 km at thicknesses of 2–3 km. The ophiolite is composed of two sub-units, the Monviso and the Lago Superiore Units (Angiboust et al., 2012). This study focuses on samples from the Lago Superiore Unit, which represents a mostly intact sequence of Tethyan sea floor, exposing slices of metamorphosed sedimentary cover, pillow lavas, basalt, gabbro, and serpentinite (Angiboust et al., 2012). Subducted to depths of about 80 km, P - T estimates for the mafic rocks of the Lago Superiore Unit put peak conditions at 550°C and 2.6–2.7 GPa (Figure 2; Angiboust et al., 2012; Groppo & Castelli, 2010).

Seven samples (Table 1) were selected from the Monviso meta-ophiolite. One sample was collected from the serpentinite sole. Three samples were collected from the overlying Mg-Al metagabbro section. One sample of Fe-Ti metagabbro was collected from the top of the gabbroic unit. Two samples of metamorphosed basalt were collected. These samples were chosen to characterize the different lithologic units of the ophiolite following subduction zone metamorphism under high P - T conditions.

Table 1
Descriptions of Western Alps Ophiolite Samples

Alpine samples	Location	Ophiolite	Lithology	Metamorphic facies	Texture	Mineralogy	Latitude	Longitude	IGSN
H17- B814A02	Western Alps	Chenaillet	Gabbro	Sub-greenschist	Coarse-grained, undeformed	Ab + Cpx (Aug) + Chl + Ep + Amp (Tr-Act) + Prh	44°53'51.93"N	6°43'54.46"E	EXT00007L
H17- B815B02		Chenaillet	Gabbro	Sub-greenschist	Coarse-grained, undeformed	Ab + Cpx (Aug) + Chl + Ep + Amp (Tr-Act)	44°53'52.35"N	6°44'4.93"E	EXT00007O
H17- B815C03-I		Chenaillet	Pillow basalt	Sub-greenschist	Fine-grained, undeformed	Ab + Cpx (Aug) + Chl + Ep ± Amp (Tr-Act)	44°53'54.50"N	6°44'6.69"E	EXT00007S
H17- B815C03-C		Chenaillet	Pillow basalt	Sub-greenschist	Fine-grained, undeformed	Ab + Cpx (Aug) + Chl + Ep ± Ol	44°53'54.50"N	6°44'6.69"E	EXT00007S
Q17- H816C01	Western Alps	Crête de l'Eychassier	Metagabbro	Low-grade blueschist	Coarse-grained, undeformed	Cpx (Aeg) + Ab + Amp (Gln) + Ep + Chl	44°42'2.79"N	6°58'18.31"E	EXT00006T
Q17- H818A01		Rocca Bianca	Metagabbro	Blueschist	Coarse-grained, strongly foliated	Cpx (Aeg) + Ab + Amp (Gln) + Ep + Chl + Ph	44°39'55.72"N	6°57'30.97"E	EXT000072
Q17- H818D01		Rocca Bianca	Metagabbro	Blueschist	Coarse-grained, weakly foliated	Cpx (Aeg) + Amp (Gln) + Ab + Ep + Chl + Ph + Ttn + Ap	44°40'21.46"N	6°57'30.02"E	EXT000076
Q17- H817C01		Bric Bouchet	Metagabbro	Blueschist	Coarse-grained, undeformed	Ab + Cpx (Aeg) + Ep + Amp (Gln) + Chl + Ttn + Ap + Ph	44°49'12.03"N	7°0'52.49"E	EXT00007Y
M17- B810A01	Western Alps	Monviso	Metabasalt	Eclogite	Fine-grained, weakly foliated	Cpx (Omp) + Ep + Chl + Ab + Amp (Gln + Tr-Act) + Opx	44°39'35.68"N	7°6'22.54"E	EXT00003B
M17- B808D03		Monviso	Metabasalt	Eclogite	Fine-grained, weakly foliated	Amp (Gln + Tr-Act) + Chl + Ab + Cpx (Omp) + Ep + Ph + Cal + Opx	44°41'32.89"N	7°5'13.76"E	EXT00003A
M17- B808B03		Monviso	Mg-Al metagabbro	Eclogite	Medium-grained, strongly foliated	Grt + Cpx (Omp) + Ep + Chl + Ab + Bt + Ph + Rt + Amp (Gln + Tr-Act)	44°41'31.33"N	7°5'18.34"E	EXT000033
M17- B819A01		Monviso	Mg-Al metagabbro	Eclogite	Coarse-grained, weakly foliated	Cpx (Omp) + Grt + Ep + Chl + Amp (Gln + Tr-Act) + Rt	44°41'34.98"N	7°5'25.54"E	EXT00007T
M17- B819A02		Monviso	Mg-Al metagabbro	Eclogite	Coarse-grained, undeformed	Cpx (Omp) + Grt + Ep + Chl + Amp (Gln + Tr-Act) + Rt	44°41'34.58"N	7°5'23.02"E	EXT00007U
M17- B808C01		Monviso	Fe-Ti metagabbro	Eclogite	Coarse-grained, undeformed	Grt + Cpx (Omp) + Ep + Chl + Ab + Ph + Ttn + Rt + Ap + Amp (Gln + Tr-Act)	44°41'23.74"N	7°5'22.66"E	EXT000036
M17- B808A01		Monviso	Serpentinite	Eclogite	Strongly foliated	Srp (Atg) + Ol	44°41'53.78"N	7°5'35.28"E	EXT000030

Note. Mineral abbreviations after Whitney and Evans (2010).

3. Methods

3.1. Sample Preparation and Bulk Rock Chemical Measurements

Approximately 50 g of rock was powdered for bulk rock geochemical measurements at the Washington State University GeoAnalytical Lab. Bulk rock major and trace element compositions were measured at the Washington State University GeoAnalytical Lab by X-ray fluorescence following sample fusion with dilithium tetraborate ($\text{Li}_2\text{B}_4\text{O}_7$) and inductively coupled plasma-mass spectrometry (ICP-MS) following acid dissolution, respectively.

Bulk rock halogen measurements were made using splits of the same rock powders. In order to remove potential surficial halogen contamination, the powders were washed five times in ultra-pure (18 m Ω) deionized water and oven-dried overnight. Halogens were extracted from ~ 2 g of powder (samples or reference materials, BCR-2 and BHVO-2) by pyrohydrolysis at the University of Texas at Austin (UT Austin). Halogens are released from the samples during heating with a gas torch and trapped in a water vapor stream, which is condensed and collected in a 20 mM NaOH solution (e.g., Schnetger & Muramatsu, 1996). Samples from the Western Alps melted completely during pyrohydrolysis. However, it was difficult to achieve 100% melting in the reference basalts BCR-2 and BHVO-2. To ensure complete sample fusion and halogen extraction from the reference materials, approximately 0.5 g of reagent grade V_2O_5 flux was added to BCR-2 and BHVO-2 samples.

Following pyrohydrolysis, F and Cl concentrations are measured by ion chromatography (IC) using a Dionex Integrion HPIC System at UT Austin. Detection limits are 0.05 $\mu\text{g/g}$ for both F and Cl. Using GeoReM preferred values for BCR-2 and BHVO-2, F yields average 92% (range = 86%–98%) and 85% (range = 78%–93%), respectively, and Cl yields average 78% (range = 69%–86%) and 71% (range = 66%–76%), respectively (Table S1 in Supporting Information S2).

Br and I concentrations in Alpine samples were measured using a Thermo Scientific Element 2 HR-ICP-MS at UT Austin. Method detection limits for Br and I are 0.35 and 0.10 ng/g, respectively. Based on GeoReM preferred values for Br in BCR-2 and BHVO-2, Br yields average 82% (range = 66%–99%) and 68% (range = 60%–77%), respectively (Table S1 in Supporting Information S2). The addition of V_2O_5 to the reference materials resulted in an I blank. The blank was removed by heating the reagent to $\sim 600^\circ\text{C}$ for ~ 16 hr. Iodine concentrations in BCR-2 and BHVO-2 standards (prepared with heat-treated reagent and without any reagent) average 26 and 63 ng/g, respectively (Table S1 in Supporting Information S2). Iodine concentrations of these reference materials range dramatically between publications (from <17 to >100 ng/g in BCR-2 and from <16 to >350 in BHVO-2; Michel & Villemant, 2003; Sekimoto & Ebihara, 2017). However, the measurements reported in this study are in close agreement with the GeoReM preferred value for BCR-2 (20 ng/g I) and Kendrick et al.'s (2018) reported BHVO-2 value (70 ± 4 ng/g).

3.2. In Situ Measurements

Mineral compositions, in situ halogen content, and mineral modal abundances were measured on a subset of samples ($n = 4$) using electron probe microanalysis (EPMA) techniques with a JEOL JXA-8200 electron microprobe at UT Austin. The operating conditions for quantitative analyses were set to 15 kV acceleration voltage, 20 nA beam current, and 5 μm spot size. On-peak counting times were 10–20 s for Na, Mg, Si, Al, Ni, Fe, Mn, K, Ti, Ca, and Cr; and 60 s for Cl and F. Scapolite and hornblende standards were used for quantification of Cl and F concentrations, respectively. The mean atomic number background correction method was used for all elements (Donovan & Tingle, 1996; Donovan et al., 2011, 2016). The detection limit for F and Cl varies by phase from 15–270 $\mu\text{g/g}$ to 90–111 $\mu\text{g/g}$, respectively. An average of 5 measurements were made per grain of each mineral, with 3–11 grains measured per sample. All elements were analyzed on all standards and all standards were measured at the beginning and end of every analytical run. Modal abundances are estimated using EDS mapping techniques. Mineral phases are defined by combining pixels with similar X-ray intensities across multiple elements. Identified phases are verified using quantitative analyses and petrography. The modal abundance percentages of each phase are then calculated using the number of pixels assigned to that phase relative to the total number of pixels included in the mapped area.

4. Results

4.1. Bulk Rock Halogen Abundances

4.1.1. Chenaillet Ophiolite

Bulk rock halogen concentrations are reported in Table 2 and Figures 3 and 4. Fluorine concentrations in all Chenaillet samples range from 46 to 164 $\mu\text{g/g}$ and average of 122 $\mu\text{g/g}$. Basaltic samples contain more F than the gabbroic samples, averaging 160 $\mu\text{g/g}$ relative to 84 $\mu\text{g/g}$. Chlorine concentrations range from 11 to 71 $\mu\text{g/g}$ with an average Cl concentration of 29 $\mu\text{g/g}$. On average, the gabbroic samples contain four times more Cl (47 $\mu\text{g/g}$) than the basaltic samples (11 $\mu\text{g/g}$). Bromine contents range from 54 to 112 ng/g and average 82 ng/g . Bromine concentrations in gabbros (102 ng/g) are significantly higher, on average, than in basalts (62 ng/g). Iodine concentrations range from 65 to 131 ng/g with an average concentration of 98 ng/g . Similar to Cl and Br, average I concentrations are higher in gabbroic (119 ng/g) than in basaltic (76 ng/g) samples. Bulk rock major and trace element compositions are reported in Table S2 of Supporting Information S2. Bulk rock data record a positive correlation between F content (in $\mu\text{g/g}$) and P_2O_5 and TiO_2 content (in wt%). No trends are observed between the contents of the other halogens (Cl, Br, I) and major or trace elements (including P_2O_5 , TiO_2 , K_2O , Ba or Rb) in Chenaillet samples.

4.1.2. Queyras Ophiolites

Metagabbro samples from the Queyras region contained between 44 and 125 $\mu\text{g/g}$ F, 9–29 $\mu\text{g/g}$ Cl, 51–89 ng/g Br, and 52–71 ng/g I. Halogen concentrations in these samples average 74 $\mu\text{g/g}$ F, 19 $\mu\text{g/g}$ Cl, 70 ng/g Br, and 63 ng/g I. Samples from the ophiolite, Crête de l'Eychassier, experienced medium P - T blueschist facies conditions and, with the exception of I, tended toward lower halogen concentrations relative to other samples from the Queyras region. Samples from Rocca Bianca experienced P - T conditions similar to Crête de l'Eychassier but recorded elevated concentrations of F, Cl, and highly variable amounts of Br and I relative to other Queyras samples. The sample from Bric Bouchet, the high P - T blueschist facies ophiolite, has low F and I and moderate

Table 2
Bulk Rock Halogen Concentrations in Alpine Ophiolites

Sample	Location	Ophiolite	Type	F ($\mu\text{g/g}$)	Cl ($\mu\text{g/g}$)	Br (ng/g)	I (ng/g)	F/Cl	Br/Cl ($\times 10^{-3}$)	I/Cl ($\times 10^{-3}$)
Low P - T Chenaillet ophiolite samples										
H17-B814A02	Sub-greenschist	Ch	Gabbro	46	71	112	131	0.7	1.6	1.8
H17-B815B02	Sub-greenschist	Ch	Gabbro	122	23	92	107	5.4	4.0	4.7
H17-B815C03-I	Sub-greenschist	Ch	Pillow basalt	156	11	54	87	14.6	5.0	8.2
H17-B815C03-C	Sub-greenschist	Ch	Pillow basalt	164	12	71	65	13.3	5.8	5.3
Medium P - T Queyras region samples										
Q17-H816C01	Med-T blueschist	CE	Metagabbro	56	9	61	69	6.5	7.1	8.0
Q17-H818A01	Med-T blueschist	RB	Metagabbro	70	22	51	60	3.2	2.4	2.8
Q17-H818D01	Med-T blueschist	RB	Metagabbro	125	29	89	71	4.4	3.1	2.5
Q17-H817C01	High-T blueschist	BB	Metagabbro	44	16	79	52	2.8	4.9	3.3
High P - T Monviso ophiolite samples										
M17-B810A01	Eclogite	MV	Metabasalt	280	8	54	72	33.2	6.4	8.6
M17-B808D03	Eclogite	MV	Metabasalt	63	6	34	78	9.8	5.4	12.2
M17-B808B03	Eclogite	MV	Metagabbro	47	8	45	74	5.6	5.2	8.7
M17-B819A01	Eclogite	MV	Metagabbro	10	9	39	69	1.0	4.1	7.3
M17-B819A02	Eclogite	MV	Metagabbro	21	7	33	64	3.19	5.0	9.7
M17-B808C01	Eclogite	MV	Metagabbro	31	9	44	64	3.44	4.9	7.2
M17-B808A01	Eclogite	MV	Metaserpentinite	0	47	344	126	0.01	7.3	2.7

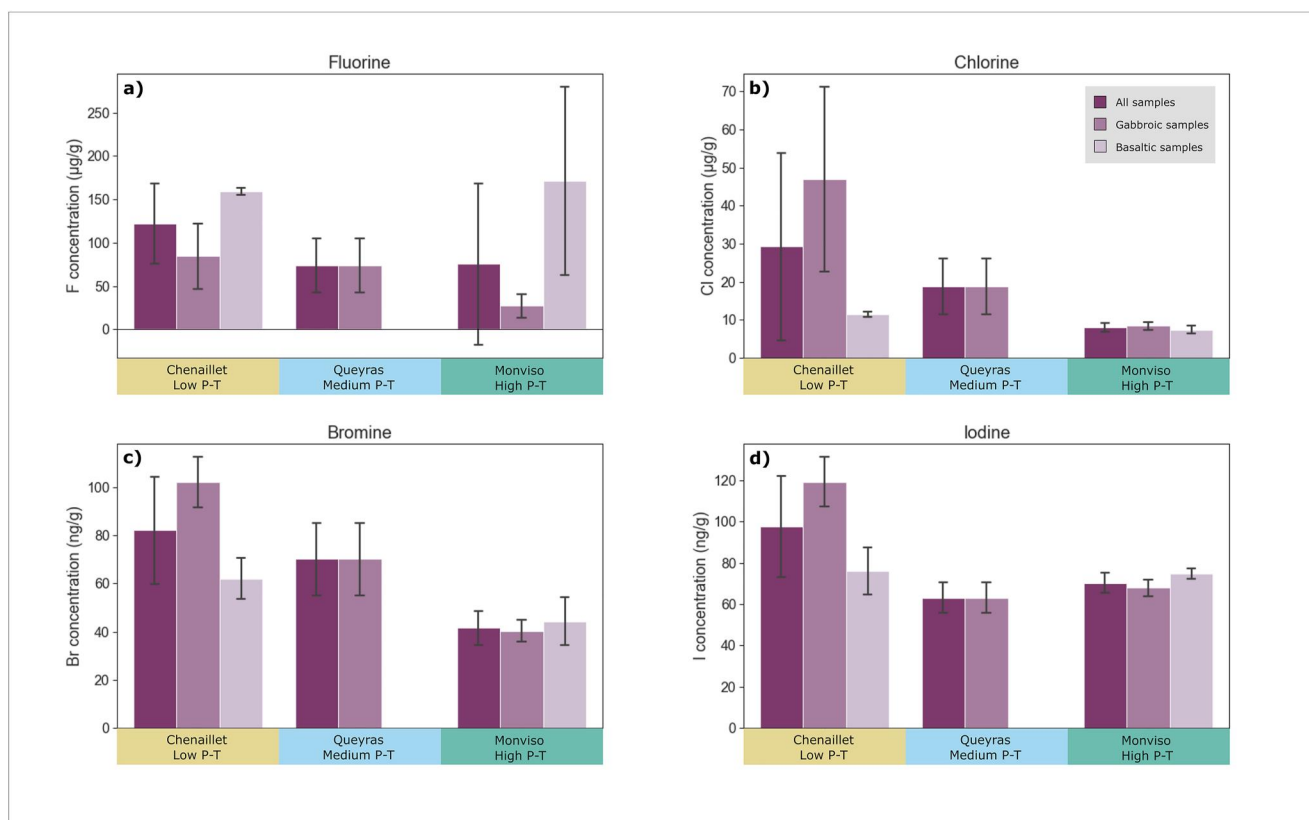


Figure 3. Bulk rock halogen data from mafic Alpine samples considered in this study. Plots display halogen content versus locality (metamorphic grade). The height of each bar represents the mean value of samples in that population, with error bars representing 1 standard deviation (1σ). In each metamorphic grade, the first bar (dark purple) represents data from all samples, including basaltic and gabbroic lithologies. The second bar (medium purple) shows data only from gabbroic samples. The third bar (light purple) shows data from basaltic samples. Note that there are no basaltic samples from the Queyras (Medium $P-T$) Region. (a) F versus locality demonstrates the highly variable F contents with overlapping values across metamorphic grade. (b) Cl versus locality shows low- $P-T$ gabbroic samples contain more Cl than their basaltic counterparts and Cl abundances decrease with increasing metamorphic grade. (c) Br versus locality shows similar trends to (b), with higher Br concentrations in low-grade gabbros and with abundances that decrease with increasing metamorphic grade. (d) I versus locality reveals elevated I contents in low- $P-T$ gabbros relative to basalts; I abundances decrease between low- and medium-grade sample sets and remain relatively unchanged from medium- to high-grade sample sets.

amounts of Cl and Br compared to the other blueschist samples. The data from this study do not indicate meaningful halogen loss between medium- and high-temperature blueschist conditions (Table 2). Queyras samples display weak correlations between F content and P_2O_5 and TiO_2 . Elevated F and Cl contents are associated with higher FeO compositions. While K_2O , Ba, and Rb abundances are elevated in Queyras samples relative to other localities, no concomitant deviation in halogen (F, Cl, Br, or I) content is observed.

4.1.3. Monviso Ophiolite

Bulk rock F concentrations in all mafic samples from Monviso range from 10 to 280 $\mu\text{g/g}$, and average 75 $\mu\text{g/g}$. Chlorine concentrations range from 6 to 9 $\mu\text{g/g}$ and average 8 $\mu\text{g/g}$. Bromine concentrations range from 33 to 54 ng/g and average 42 ng/g . Iodine concentrations range from 64 to 78 ng/g and average 70 ng/g . Bulk rock major and trace element results (Table S2 in Supporting Information S2) from Monviso samples show that positive correlations between F and P_2O_5 , TiO_2 , and FeO content continue into the eclogite-facies. Chlorine abundances are not correlated with the abundances of major or trace elements. Monviso samples, particularly among the metagabbroic suite, record weak, positive correlations between Br and FeO, P_2O_5 , TiO_2 , K_2O , and Na_2O content and between I and P_2O_5 , Na_2O , and Sr contents.

When gabbroic and basaltic samples are considered separately, the impact of lithology on the halogen content is less distinct than in the low-grade samples from Chenaillet. Basaltic samples from Monviso contain more F than gabbroic samples, averaging 171 $\mu\text{g/g}$ and 27 $\mu\text{g/g}$, respectively. For Cl, Br, and I, the variations in the

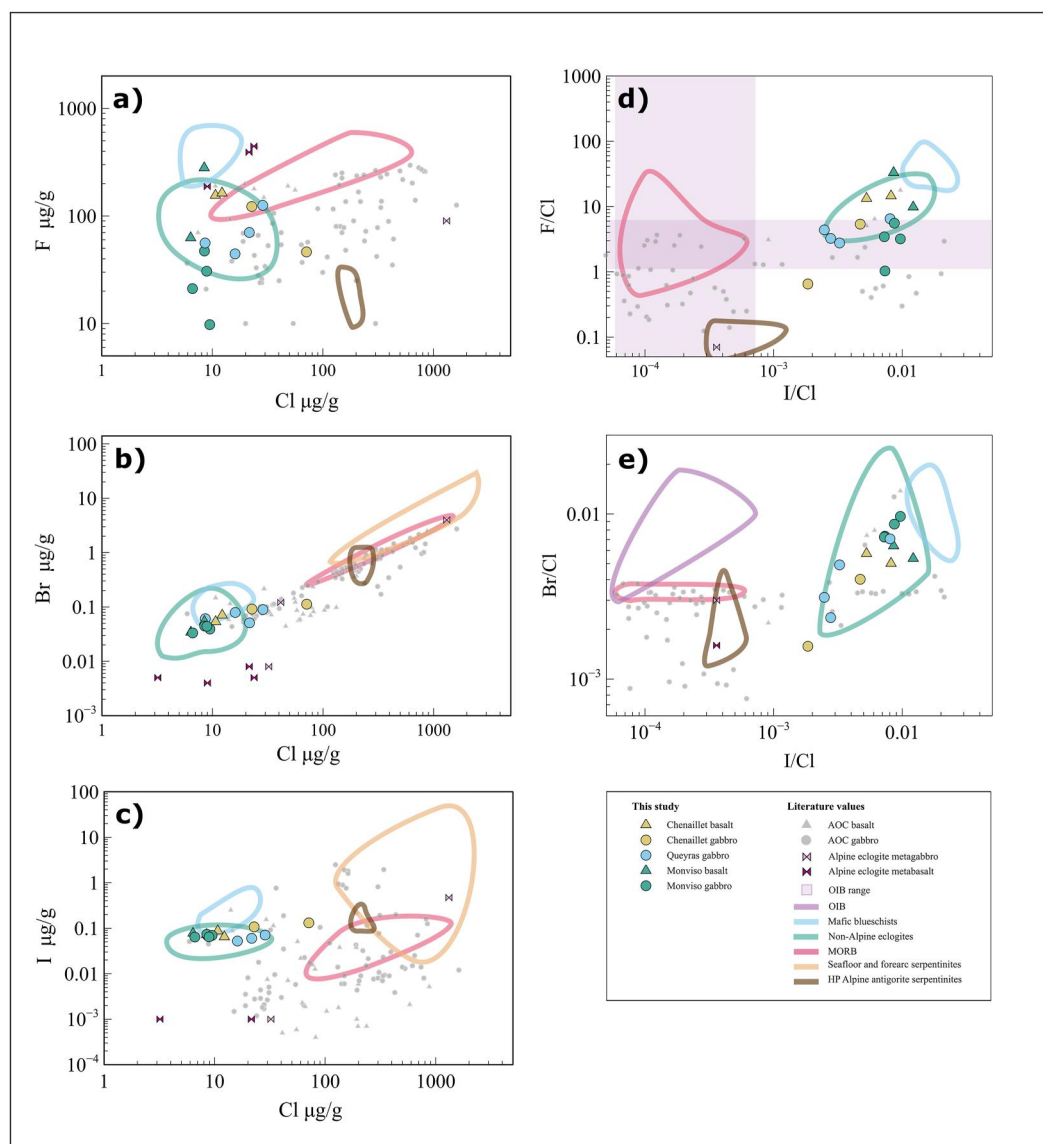


Figure 4. Halogen concentrations and ratios from this study compared with literature data from different geologic reservoirs and lithologies. (a) F versus Cl concentrations are not correlated with Alpine samples. (b) Br versus Cl concentrations show strong positive correlations across all Alpine samples. (c) I versus Cl concentrations are not correlated in Alpine samples. (d) F/Cl versus I/Cl ratios show a weak correlation between F and I. (e) Br/Cl versus I/Cl ratios show a correlation between Br and I. Alpine eclogites have elevated Br/Cl and I/Cl ratios relative to lower-grade samples, suggesting the preferential loss of Cl relative to Br and I. The halogen contents and ratios of other rock types are shown for reference: AOC—Beaudoin et al. (2022), Chavrit et al. (2016), Kendrick (2019a, 2019b); Alpine eclogite metagabbro—Hughes et al. (2018); Alpine eclogite metabasalt—Hughes et al. (2018); OIB range—F/Cl data from Hauri (2002), I/Cl data from Kendrick, Jackson, et al. (2015); OIB—Kendrick, Jackson, et al. (2015); mafic blueschists—Pagé et al. (2016); non-Alpine eclogites—Beaudoin et al. (2022); MORB—le Roux et al. (2006), Kendrick et al. (2012); seafloor and forearc serpentinites—Kendrick et al. (2013); HP Alpine antigorite serpentinites—John et al. (2011).

concentration between basaltic and gabbroic eclogites are nearly imperceptible, with average values of 7–8 $\mu\text{g/g}$ Cl, 44 to 40 ng/g Br, and 75 to 68 ng/g I, respectively.

One serpentinite sample was selected from Monviso and analyzed for halogen content. With concentrations of <1 $\mu\text{g/g}$ F, 47 $\mu\text{g/g}$ Cl, 344 ng/g Br, and 126 ng/g I, it is chemically distinct from the mafic samples that experienced similar metamorphic conditions (Table S2 in Supporting Information S2).

4.2. In Situ Halogen Measurements

A subset of samples was selected for in situ quantitative analyses of mineral compositions via EPMA. Representative samples of each metamorphic facies were selected based on petrographic observations: one low-grade gabbro from the sub-greenschist facies Chenaillet ophiolite (H17-B814A02), one metagabbro from the blueschist facies Rocca Bianca ophiolite of the Queyras region (Q17-H818D01), and two metagabbros from the eclogite facies Monviso ophiolite (M17-B808D03 and M17-B808C01). Major element mineral compositions and in situ halogen concentrations (F and Cl) are reported in Table S4 in Supporting Information S2. Estimated modal abundances from EDS mapping and calculations of bulk rock F and Cl contents are recorded in Table S3 of Supporting Information S2. EDS maps and corresponding thin section photomicrographs are shown in Figure 5.

4.2.1. Chenaillet Ophiolite

In order to establish a baseline for halogen contents in mafic Alpine oceanic crust following magmatic emplacement and seafloor alteration, the compositions of minerals in a gabbro sample (H17-B814A02) from the Chenaillet ophiolite were analyzed. This sample is characterized by a magmatic assemblage of clinopyroxene and plagioclase, which are variably overprinted by secondary alteration phases, including amphibole, chlorite, epidote, and minor prehnite. Clinopyroxenes have an augite composition, with X_{Mg} ($=Mg/[Mg + Fe]$) of 0.77 and CaO and Al₂O₃ contents of 21.3 wt% and 1.8 wt%, respectively. Feldspars are albitic in composition. Amphiboles are actinolite, with X_{Mg} of 0.70 and Al₂O₃ content of 4.2 wt%. Chlorite in this sample is an intermediate member of the chamosite-clinochlore series, containing equal portions of MgO and FeO at 19.3 wt% MgO and 19.0 wt%, respectively.

Clinopyroxenes contain no detectable F or Cl (Table S4 in Supporting Information S2). Measurements of halogen concentrations in actinolite record low concentrations (approximately 1,000 µg/g F and 300 µg/g Cl) and are characterized by relatively high analytical uncertainties (Table S4 in Supporting Information S2). Despite the uncertainties, the reported F and Cl contents of these amphiboles are consistent with the ranges reported by other authors. Using SIMS analyses, actinolite from the Chenaillet ophiolite has been reported to have F contents between 36.8 and 132.0 µg/g and Cl contents between 17.2 and 652 µg/g (Debret et al., 2016). Similarly, studies of halogen content in secondary amphiboles from seafloor metagabbros report 1,000 µg/g F (e.g., Coogan et al., 2001) and 100–500 µg/g Cl (e.g., Kendrick, Honda, & Vanko, 2015). All other phases in this sample contain Cl in concentrations that are below the detection limit. Other phases that contain F include prehnite (300 µg/g), albite (400 µg/g), epidote (400–1,000 µg/g), and chlorite (300 µg/g).

4.2.2. Queyras Ophiolites

Mafic samples from the Queyras region represent oceanic crust, similar to the material preserved in the Chenaillet ophiolite that experienced prograde subduction and recrystallization under blueschist facies conditions. The mineral compositions and modal abundances of one representative blueschist metagabbro (Q17-H818D01), collected from the Rocca Bianca ophiolite, are reported in Tables S3 and S4 in Supporting Information S2, respectively. This sample is composed of clinopyroxene, sodic amphibole, albite, epidote, chlorite, phengite, titanite, and apatite. Clinopyroxenes are Na-rich (at 12.0 wt% Na₂O) with an aegirine-augite composition that contains significantly more FeO (22 wt%) and Al₂O₃ (4.8 wt%) and less MgO (2.9 wt%) and CaO (3.7 wt%) than augites from Chenaillet. Feldspars have an albitic composition. Amphiboles show a ferro-glaucophane composition, with Na₂O contents of 7.6 wt%, Al₂O₃ contents of 3.7 wt%, and MgO and FeO contents of 8.3 wt% and 21.0 wt%, respectively. Epidotes in this sample are significantly more Fe rich than those analyzed from the Chenaillet ophiolite, with FeO contents of 14.0 wt%. Similarly, the blueschist sample contains chlorites that are more Fe-rich than those measured in the sub-greenschist facies Chenaillet sample. The chlorites measured in the Queyras sample are intermediate members of the chamosite-clinochlore series with MgO and FeO contents of 17.9 wt% and 22.0 wt%, respectively. White mica, present as phengite, is observed in this sample. The phengite contains a high amount of Si (3.3 apfu) and Al₂O₃ (27.9 wt%).

No F is detected in sodic clinopyroxene or epidote within the blueschist facies metagabbro from the Queyras region. F is measured in variable quantities within a number of phases, including sodic amphibole (200 µg/g), albite (200 µg/g), chlorite (2,300 µg/g), phengite (2,500 µg/g), titanite (1,000 µg/g), and apatite (2.9 wt%). The F contents in blueschist facies amphiboles, epidotes, and chlorites are significantly lower (by factors of 5, 2.5, and

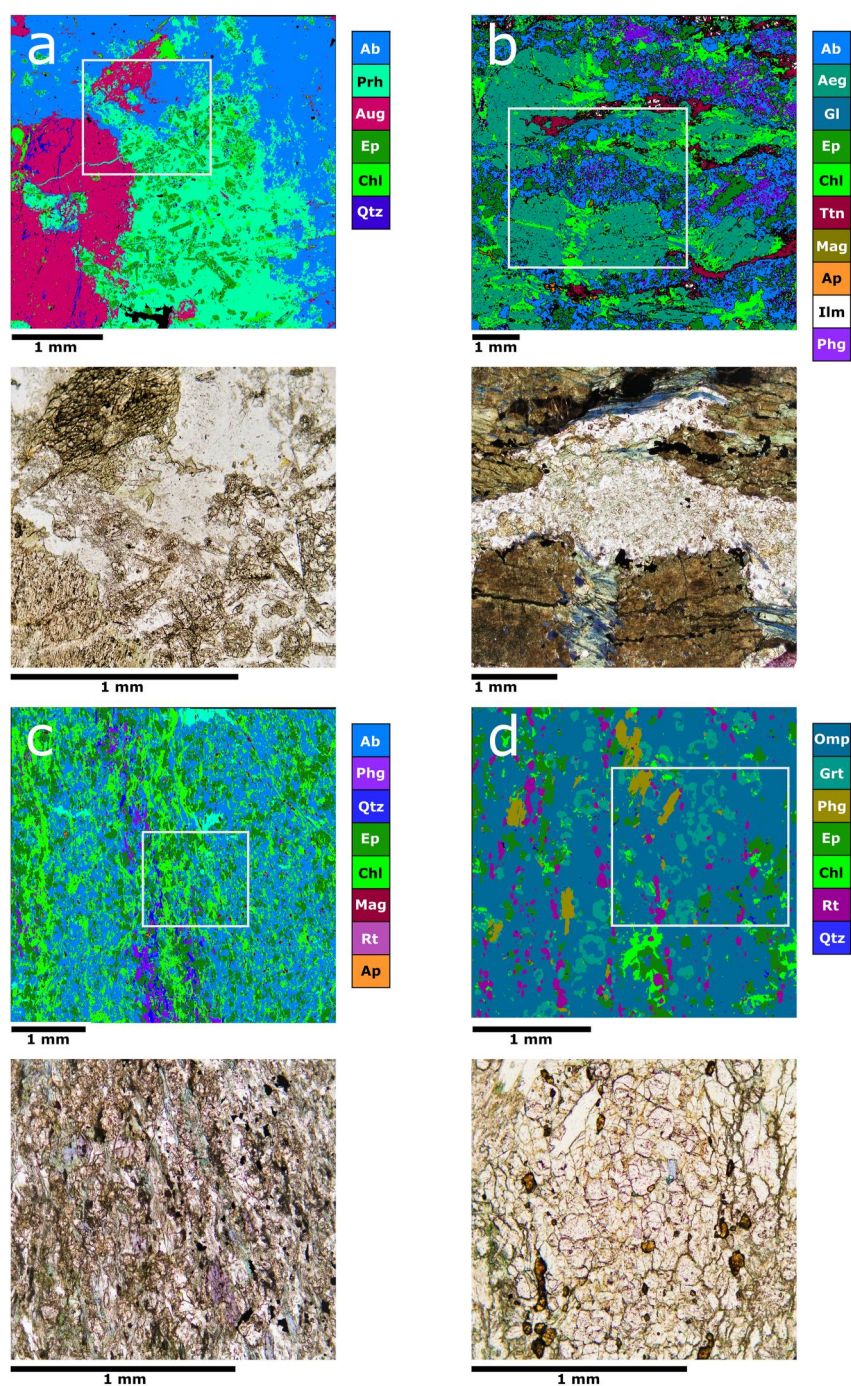


Figure 5. Paired EDS map (top) and photomicrograph (bottom) documenting texture and mineral abundance and distribution of (a) sample H17-B814A02 from the sub-greenschist facies, Chenailet ophiolite, (b) sample Q17-H818D01 from the blueschist facies, Queyras Region, (c) sample M17-B808D03 from the eclogite facies, Monviso meta-ophiolite, and (d) sample M17-B808C01 from the eclogite facies, Monviso meta-ophiolite. Mineral phases are color coded. The white square indicates the location and extent of the corresponding photomicrograph. Scale bars illustrate the relative sizes of 1 mm in each area. Mineral abbreviations: Ab (albite), Aeg (aegirine), Ap (apatite), Aug (augite), Chl (chlorite), Ep (epidote), Gl (glaucophane), Grt (garnet), Ilm (ilmenite), Mag (magnetite), Omp (omphacite), Phg (phengite), Prh (prehnite), Qtz (quartz from glass slide), Rt (rutile), Ttn (titanite).

1.3, respectively) than F contents measured in the corresponding mineral phases from the low-grade Chenaillet sample. Cl contents are at or below the detection limits for all phases in the blueschist assemblage.

4.2.3. Monviso Ophiolite

With continued subduction and prograde metamorphism beyond blueschist facies conditions, altered oceanic crust forms an eclogitic assemblage. From the Monviso ophiolite that reached eclogite-facies conditions, one metabasalt (M17-B808D03) and one metagabbro (M17-B808C01) were selected for in situ analyses. The high-pressure assemblage recorded in these samples is composed of clinopyroxene, garnet, sodic amphibole, epidote, chlorite, phengite, titanite, rutile, and apatite (Figure 5). Retrograde albite is observed in both samples. Previous work has also suggested that epidote from Monviso formed from the breakdown of lawsonite (e.g., Angiboust et al., 2012; Blake et al., 1995). Minor calcite is present around fractures in the metabasalt sample M17-B808D03, and minor biotite is observed in the metagabbro sample M17-B808C01. Clinopyroxenes have an omphacite composition, with 8.6–9.1 wt% Na₂O at 0.6 Na apfu and variable FeO contents (5.7–12.0 wt%). Garnets have a mixed composition with high almandine content and low proportions of pyrope and grossular endmembers. Amphiboles present as actinolite in the metabasalt sample, with X_{Mg} of 0.73 and Al₂O₃ contents of 2.1 wt%. In the metagabbro sample, amphiboles have a glaucophane composition with Na₂O contents of 7.1 wt%, Al₂O₃ contents of 8.0 wt%, and MgO and FeO contents of 9.1 wt% and 15.0 wt%, respectively. Monviso epidotes are less Fe-rich (7.3–9.0 wt%) than those found in the blueschist metagabbro (14.0 wt%). Chlorites have slightly elevated MgO contents and lower FeO contents than chlorites observed in the Chenaillet and Queyras samples. Phengites in Monviso samples are Si-rich (3.4–3.7 apfu) with Al₂O₃ contents ranging from 20.0 to 27.3 wt%.

In situ measurements of halogens in selected eclogite samples from the Monviso ophiolite show that amphibole, chlorite, epidote, phengite, biotite, titanite, and apatite all host variable amounts of F (Table S4 in Supporting Information S2). Quantities average 1,000 µg/g in amphibole and phengite, 1,200 µg/g in biotite, 1,800 µg/g in titanite, and 2.7 wt% in apatite. In situ F values range from 600 to 1,000 µg/g in epidote and 1,100–2,100 µg/g in chlorite. Cl contents are at or below the detection limits in all minerals analyzed. The Cl composition of actinolites from the Monviso metabasalt is approximately 100 µg/g, but given the high analytical uncertainty associated with these measurements, we consider the value to be a maximum estimate of Cl content in eclogite facies amphiboles, which is largely consistent with previous work (e.g., Debret et al. (2016) report 25–146 µg/g Cl in glaucophane from Monviso eclogites). No Cl is detected in the apatite grains, which appear to host a significant concentration of F (Table S4 in Supporting Information S2).

5. Discussion

5.1. Comparing Measured and Reconstructed Bulk Rock Abundances

Using the EPMA in situ measurements of F and Cl (Table S4 in Supporting Information S2) and the estimated mineral modal abundances, the bulk rock concentrations of F and Cl can be reconstructed (Table S3 in Supporting Information S2). These calculated bulk rock concentrations are then compared to the measured bulk rock abundances from IC and ICP-MS analyses (Table 3) for samples H17-B814A02, Q17-H818D01, M17-B808D03, and M17-B808C01. Results of this comparison show that the calculated bulk rock F concentrations are significantly higher than the measured values. Reconstructed bulk rock F concentrations result in 483 µg/g in the sample from Chenaillet, 722 µg/g in the sample from Queyras, 749 µg/g in the metabasalt from Monviso, and 164 µg/g in the metagabbro from Monviso. These values are ~10, ~6, ~12, and ~5 times larger than the measured F abundances in those samples, respectively. However, if the Monviso epidote is considered retrograde and its F contribution is removed from the reconstructed bulk F concentration, then the disparities are reduced to ~8 and ~3 times larger for the Monviso metabasalt and metagabbro, respectively. In contrast, the disparity between the reconstructed and measured bulk rock abundances is less for Cl. Reconstruction of bulk rock Cl contents using in situ data are: 47 µg/g in sample H17-B814A02, 0 µg/g in sample Q17-H818D01, 12 µg/g in sample M17-B808D03, and 0 µg/g in sample M17-B808C01. Most of these estimates are lower (except for M17-B808D03) than the measured Cl abundances: 71, 29, 6, and 9 µg/g, respectively.

Based on the comparison between methods, using reconstructed bulk rock F and Cl abundances based on in situ measurements can lead to substantial overestimation of F and slight underestimation of Cl, as illustrated in Figure 6. Reconstructed bulk rock abundances can only account for crystal lattice-hosted halogens that are present

Table 3
Summary of Bulk Rock Halogen Contents in Alpine Ophiolites

Metamorphic grade	F (μg/g)	Cl (μg/g)	Br (ng/g)	I (ng/g)
Low <i>P-T</i> Chenaillet ophiolite samples				
Range	46–164	11–71	54–112	65–131
Average	122	29	82	98
Uncertainty ^a	±74	±39	±35	±39
Medium <i>P-T</i> Queyras region samples				
Range	44–125	9–29	51–89	52–71
Average	74	19	70	63
Uncertainty	±49	±12	±24	±12
High <i>P-T</i> Monviso ophiolite samples (mafic samples only)				
Range	10–280	6–9	33–54	64–78
Average	75	8	42	70
Uncertainty	±98	±1	±7	±5

^aAll uncertainties were calculated to a 95% confidence level.

in concentrations greater than the detection limit; this may explain the discrepancy between reconstructed and measured Cl values. Portions of the Cl budget that are hosted in non-structural sites (e.g., fluid inclusions, grain boundaries, crystal defects) cannot be measured using EPMA techniques. Additionally, structural Cl-hosting in minerals may account for a non-trivial portion of the bulk rock budget, but if the concentrations are lower than the EPMA detection limits, they cannot be measured. If a conservative estimate of 0.005 wt% Cl is assumed for all analyzed hydrous phases from samples H17-B814A02, Q17-H818D01, M17-B808D03, and M17-B808C01 that had Cl concentration below the detection limits, then the reconstructed bulk rock Cl abundances become 61, 23, 27, and 9 μg/g, respectively. Generally, these values more closely agree with bulk rock measurements and demonstrate the difficulty in using in situ techniques to evaluate bulk rock abundances of low-Cl samples. A study by Urann et al. (2020) compared reconstructed (using SIMS data) and measured (via pyrohydrolysis and IC) bulk rock F and Cl concentrations in a suite of eclogites from the Raspas Complex, Ecuador. They found similar disparities between the methods. Although their F estimates were in closer agreement than in this study, they ascribe the apparent underestimation of Cl that was observed in the reconstructed data to significant amounts of Cl being hosted in non-lattice sites.

5.2. The Protolith of Alpine Metamorphic Samples

The assertion that samples of Chenaillet can be used to represent protolith material for metamorphosed Alpine ophiolites has been put forth by a number of previous studies (e.g., Debret et al., 2016; Lafay et al., 2013; Philippot et al., 1998). These authors justify their claims using mineralogical, geochemical, structural, and petrological evidence. Halogen concentrations in Chenaillet lend further support to this interpretation. On average, mafic samples from Chenaillet contain 122 ppm F, 29 ppm Cl, 82 ppb Br, and 98 ppb I (Figures 3 and 4; Table 2). These values fall within the range of values measured in mafic AOC samples by previous authors (Figure 4; Beaudoin et al., 2022; Chavrit et al., 2016; Kendrick, 2019a, 2019b). Despite this overall agreement, the Chenaillet mafic rocks contain Br abundances at the low end and I abundances at the high end of published Br and I concentration ranges of seafloor basalts and gabbros (Figure 4), perhaps indicating a different degree of seafloor hydrothermal alteration or a late-stage remobilization of halogens during obduction and deformation. Given that Cl, Br, and I are likely to be incorporated into ocean crust during more extensive hydrothermal alteration and the subsequent formation of pervasive, secondary alteration phases (Chavrit et al., 2016; Kendrick, 2019b; Kendrick, Caulfield, et al., 2020; Zhang et al., 2017), seafloor alteration in the slow-spreading Alpine Tethys basin may not have generated sufficient hydrothermal circulation to produce the heavy halogen contents that might be expected, if the prediction is based on observations of altered basalts and gabbros from more mature, fast-spreading margins.

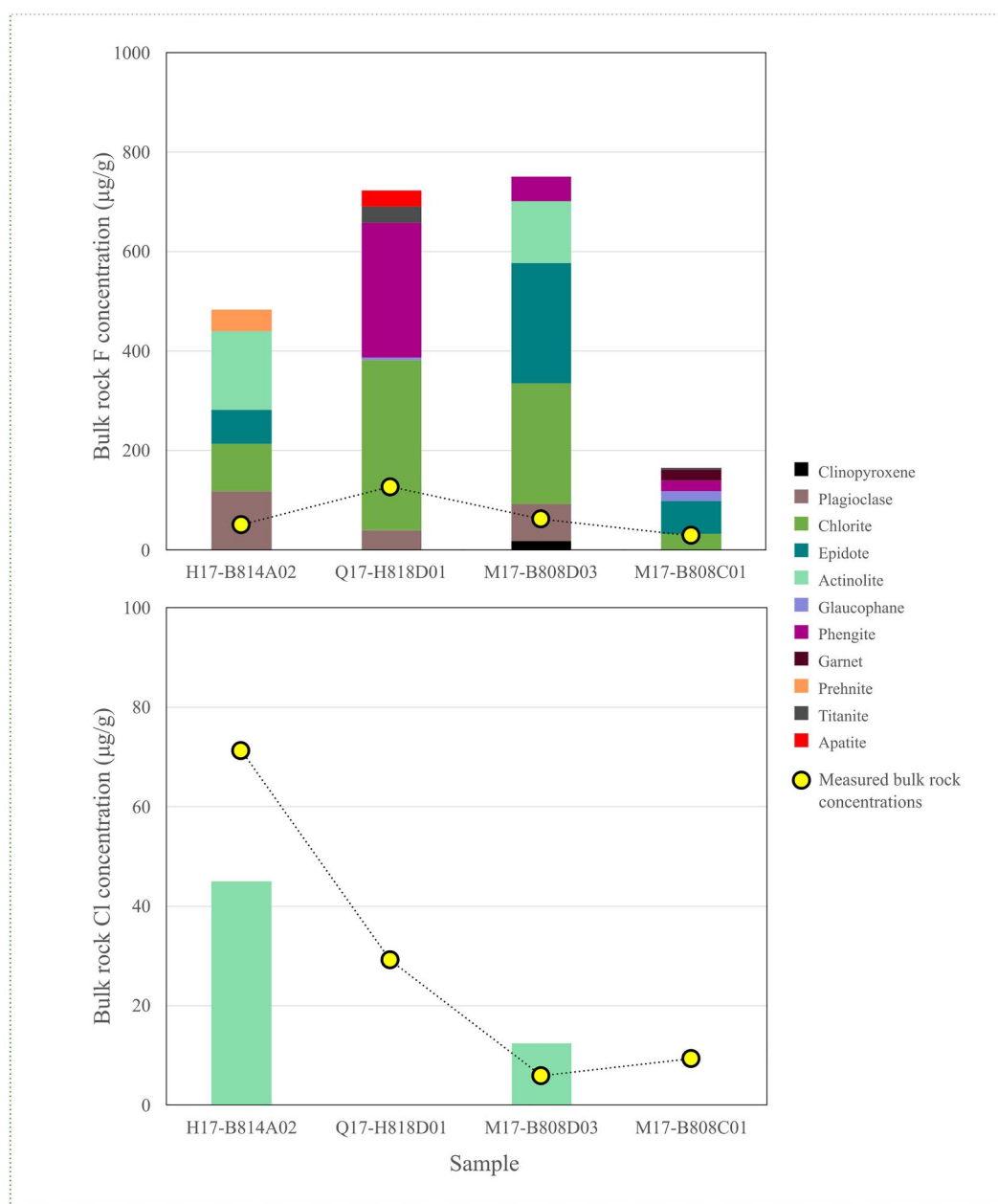


Figure 6. Diagrams showing the disparity between bulk rock values of F and Cl determined using different methods. Halogen (F and Cl) concentrations are plotted on the y-axis. Samples analyzed using in situ methods are along the x-axis with metamorphic grade increasing to the right. Bar graphs represent in situ data collected by EPMA; colored sections show the contributions from different mineral phases and how those phases change across metamorphic grade. The yellow circles connected by the dashed black line show the halogen contents that were determined using bulk rock geochemical methods.

The overlapping halogen contents of AOC and Chenaillet samples support the model that the Chenaillet ophiolite serves as an analog for unmetamorphosed Alpine Tethys seafloor and can be used to model the protolith composition of metamorphic ophiolites found throughout the Alpine orogeny. Within AOC and within the Chenaillet ophiolite, there are different lithologic components, basalts and gabbros that should be treated separately when determining changes in volatile content with increasing metamorphic grade. Seafloor hydrothermal alteration varies with depth; thus, basalts and gabbros experience disparate styles of halogen incorporation likely linked to mineralogy with more phyllosilicates in low-temperature altered basalts and amphiboles in high-temperature altered gabbros. Results indicate that basaltic samples host F in greater concentrations than

gabbroic rocks, whereas gabbros incorporate more Cl and Br (Figure 3; Beaudoin et al., 2022; Kendrick, 2019a). These variably halogen-enriched basalts and gabbros subsequently evolve along different physical and chemical trajectories during subduction zone metamorphism and devolatilization. Despite the petrologic similarities, metabasalts and metagabbros should be considered separately when estimating changes to the halogen budget.

In the following sections, halogen contents will be discussed by lithology within ophiolites from different metamorphic grades. As stated in Section 2, metabasalts from the Queyras region were deemed unsuitable for this study, largely due to metasomatic overprinting. Therefore, while changes in the halogen content in metagabbros can be compared across three ophiolites that experienced different metamorphic facies conditions, comparisons of metabasalts can only be made between Chenaillet and Monviso samples.

5.3. Halogen Behavior During Prograde Metamorphism

5.3.1. Fluorine

Fluorine contents average 160 $\mu\text{g/g}$ in Chenaillet basalts and range from 156 to 164 $\mu\text{g/g}$ (Figure 3; Table 2). These values are comparable to F abundances in previously analyzed AOC basalts (Figure 4; 170–300 $\mu\text{g/g}$ F, Kendrick, 2019a; 70–440 $\mu\text{g/g}$ F, Beaudoin et al., 2022). In Monviso metabasalts, F contents average 172 $\mu\text{g/g}$ and range from 63 to 280 $\mu\text{g/g}$, overlapping values reported in metabasalts from other eclogitic terrains (92–160 $\mu\text{g/g}$, Beaudoin et al., 2022; 188–445 $\mu\text{g/g}$, Hughes et al., 2018). Based on these results, and assuming a similar starting composition for the Chenaillet and Monviso ophiolites, F is not effectively mobilized from subducting basalts during prograde metamorphism up to eclogite facies conditions (e.g., a *t*-test does not show a statistically significant difference between Chenaillet and Monviso basalts). Ratios of F/Cl increase between subgreenschist basalts (average F/Cl = 14.0) and eclogite facies metabasalts (average F/Cl = 21.5). These ratios are consistent with averages reported for AOC basalts (F/Cl = 9.0, Beaudoin et al., 2022), non-Alpine eclogitic metabasalts (F/Cl = 17.1, Beaudoin et al., 2022), and other Alpine eclogitic metabasalts (F/Cl = 19.3, Hughes et al., 2018) (Figure 4). The increase in F/Cl with increasing metamorphic grade is consistent with the loss of Cl (statistically significant at the 90% confidence level based on a *t*-test, $p = 0.09$) relative to the retention of F during prograde subduction.

Metagabbros typically contain less F and lower F/Cl ratios than their metabasaltic counterparts (Figure 4). Fluorine values (average 74 $\mu\text{g/g}$ and range from 44 to 125 $\mu\text{g/g}$ F) in blueschist metagabbros from Queyras closely overlap those in Chenaillet gabbros, which average 84 $\mu\text{g/g}$ and range from 46 to 122 $\mu\text{g/g}$. These results suggest that, as with basalts, the F content of subducting gabbros is not prone to remobilization during prograde metamorphism, specifically up to high *P-T* blueschist facies. The F content in metagabbros from Monviso is lower, averaging 27 $\mu\text{g/g}$ and ranging from 10 to 47 $\mu\text{g/g}$ F. Hughes et al. (2018) similarly report F concentrations <100 $\mu\text{g/g}$ for other Alpine eclogitic metagabbros, including at Monviso. Debret et al. (2016) also report low calculated bulk F concentrations in Monviso metagabbros (10–16 $\mu\text{g/g}$) and Queyras metagabbros (27–67 $\mu\text{g/g}$); however, they reported much higher F concentrations in Chenaillet metagabbros (42–657 $\mu\text{g/g}$) than reported in this study. The high F concentrations of Debret et al. (2016) are calculated based on mineral composition and modal abundance. Debret et al. (2016) report three different amphibole generations at Chenaillet with a large range in F concentrations; therefore, depending on the amphibole F concentration used, high bulk F contents are calculated. Using measured bulk concentrations, we find that F/Cl ratios are relatively constant among Alpine gabbros and metagabbros: 3.0 in Chenaillet, 4.2 in Queyras, and 3.3 in Monviso. The slight increase in F/Cl between gabbroic samples from Chenaillet to Queyras was consistent with F retention and Cl loss. A similar increase in the ratio from Queyras to Monviso is expected as Cl loss continues (statistically significant at the 90% confidence level based on a *t*-test, $p = 0.09$); however, it is masked by a drop in F content (statistically significant at the 90% confidence level based on a *t*-test, $p = 0.07$). The reduction in the F content of Monviso metagabbros relative to their Chenaillet-like protolith could be the result of F loss during dehydration, protolith variations, or non-representative sampling.

Given the ability of F to substitute into different structural sites, its proclivity for forming strong bonds, and the abundance of potential host phases in mafic lithologies (e.g., Hughes et al., 2018; Pagé et al., 2016; Urann et al., 2017), F is expected to behave compatibly during metamorphic dehydration reactions and be retained in the solid slab residue to depths of arc magma genesis and mantle recycling. Ratios of F/Cl in all Monviso eclogites (F/Cl range = 1–33; average F/Cl = 9.4) overlap with values reported for OIBs (F/Cl \approx 2–17) (Hauri, 2002). This fluid-immobile behavior has been predicted and observed in previous studies (e.g., Barnes et al., 2018; Beaudoin

et al., 2022; Hughes et al., 2018; John et al., 2011; Pagé et al., 2016; Straub & Layne, 2003). In contrast, Debret et al. (2016) report large F loss (~90%) in metagabbros by eclogite facies, largely due to the high initial calculated F concentrations of Chenaillet metagabbros. No correlations are observed between F contents and the abundances of Cl, Br, or I in this study.

5.3.2. Chlorine

Limited variation is present in the Cl contents of basalts and metabasalts from Alpine ophiolites in this study. Chlorine contents in metabasalts from Chenaillet average 12 $\mu\text{g/g}$ and range from 11 to 12 $\mu\text{g/g}$. Concentrations decrease by ~35% between sub-greenschist facies and eclogite facies, with metabasalts from the Monviso ophiolite averaging 7 $\mu\text{g/g}$ and ranging from 6 to 8 $\mu\text{g/g}$ Cl (Figure 3; Table 3), and overlap with other reported Alpine eclogitic metabasalts (3–24 $\mu\text{g/g}$ Cl, Hughes et al., 2018). The low initial Cl composition of the Chenaillet basalts is consistent with Cl contents measured in AOC basalts from drill cores (Figure 4; Beaudoin et al., 2022; Chavrit et al., 2016), which systematically incorporate less Cl than their high-T, amphibole-bearing, altered gabbroic counterparts. The lower initial Cl abundances observed in basalts cause them to be less influential in controlling the Cl budget of subducting AOC than gabbros.

On average, Chenaillet gabbros contain 47 $\mu\text{g/g}$ Cl, ranging from 23 to 71 $\mu\text{g/g}$ (Figure 4). The average Cl content decreases by ~60% between sub-greenschist and blueschist facies samples, with metagabbro samples from Queyras ophiolites averaging 19 $\mu\text{g/g}$ and ranging from 9 to 29 $\mu\text{g/g}$ Cl. Compared to the blueschist facies metagabbros from Queyras ophiolites, the eclogite facies metagabbros from the Monviso ophiolite contain ~55% less Cl. Eclogitic metagabbros show very little variation in Cl concentration, averaging 8 $\mu\text{g/g}$ Cl and ranging from 7 to 9 $\mu\text{g/g}$. Other work documents slightly higher Cl concentrations in Alpine eclogitic metagabbros (32–42 $\mu\text{g/g}$ Cl, minus one outlier, Hughes et al., 2018; 71–79 $\mu\text{g/g}$ Cl, Debret et al., 2016).

The precipitous loss of Cl from low- to medium- to high-grade mafic samples suggests efficient remobilization of Cl during prograde metamorphism. Numerous previous fluid inclusion studies on metasedimentary and metamafic rocks along a similar transect as to those in this study report moderately to high saline contents (Agard et al., 2000; Herviou et al., 2021; Nadeau et al., 1993; Philippot & Selverstone, 1991; Philippot et al., 1998). With increasing metamorphic grade, there is an overall decrease in fluid inclusion salinity (Herviou et al., 2021). High salinity in the metamafic samples are interpreted as reflecting an inherited seafloor signature from hydrothermal alteration, with progressive Cl loss during subduction (Herviou et al., 2021). These observations from fluid inclusion chemistry mimic the chlorine concentration of the bulk rock. Based on this dataset (summarized in Table 3), the removal of >70% of the initial Cl entering the subduction zone in gabbroic ocean crust is expected to occur between the trench and eclogite facies conditions, with the most significant reduction occurring prior to blueschist facies conditions. Chlorine's mobile behavior is attributed to its hydrophilic nature (e.g., Manning, 2004) and the destabilization of major host phases (particularly amphibole) with increasing metamorphic conditions. Previous studies have estimated that ~50% (Debret et al., 2016) to >90% of Cl (Barnes et al., 2018; Beaudoin et al., 2022; Hughes et al., 2018; Ito et al., 1983; Straub & Layne, 2003) is removed from the downgoing slab prior to reaching depths of arc magma genesis. This behavior of significant loss is expected to extend to the other heavy halogens (Br and I).

5.3.3. Bromine

Bromine contents in Chenaillet basalts average 62 ng/g and range from 54 to 71 ng/g (Figure 3). The Monviso metabasalts average 44 ng/g Br and range from 34 to 54 ng/g. Similar to Cl loss from basalts, this amounts to a Br loss of ~30% from subducting basalts prior to depths of ~80 km. The concomitant loss of Br and Cl resulted in ratios that are largely unchanged between low-grade basalts (Br/Cl averages 5.4×10^{-3}) and HP metabasalts (Br/Cl averages 5.9×10^{-3}). The slight increase in Br/Cl ratios with metamorphic grade is consistent with Cl being more efficiently devolatilized from the mafic slab than Br.

The systematic loss of Br with increasing peak metamorphic conditions is apparent when investigating the more complete gabbroic dataset (Figures 3 and 4). In the Chenaillet ophiolite, gabbros average 102 ng/g Br with a Br/Cl ratio averaging 2.8×10^{-3} , well within the range of published values for AOC gabbros (Figure 4). Within the Queyras ophiolites, the Br content of metagabbros drops by ~30% to an average of 70 ng/g, with the average Br/Cl ratio increasing to 4.4×10^{-3} . From blueschist to eclogite facies conditions, the Br concentration in Monviso metagabbros decreases by ~40% to an average of 40 ng/g and 4.8×10^{-3} Br/I. The increase in Br/Cl ratios

between Chenaillet gabbros and Queyras metagabbros, relative to the increase between Queyras and Monviso metagabbros, could point to an early expulsion of Cl from the slab prior to reaching blueschist facies, whereas Br devolatilization rates remain more stable.

Overall, >60% of initial Br is lost from the gabbroic section of the subducting slab (statistically significant at the 90% confidence level based on a *t*-test, $p = 0.08$). Bromine, like Cl, is expected to devolatilize during prograde metamorphism. A strong, positive correlation is observed between Cl and Br content in these samples and is a well-documented trend within various relevant geologic reservoirs (Figure 4), including AOC basalts and gabbros (Chavrit et al., 2016; Kendrick, 2019a, 2019b), MORB glasses (Kendrick et al., 2012), seafloor and forearc serpentinites (Kendrick et al., 2013), arc volcanics (John et al., 2011), and marine sedimentary pore fluids (Muramatsu et al., 2007). Due to its large ionic size, it is unlikely that Br would substitute into the structural sites that are typically occupied by smaller ions in progressively more anhydrous mineral assemblages. With the collapse of pore spaces and few phases that can incorporate Br, it is efficiently removed from the subducting slab prior to eclogite facies conditions. Previous studies estimate that <10% of total Br entering a subduction zone is recycled to the upper mantle (Beaudoin et al., 2022; Kendrick, Jackson, et al., 2014). When considering only the Br budget of subducted mafic lithologies (excluding Br contributions to the subduction zone from sedimentary rocks and serpentinites), a significant portion of the initial Br content is retained in the subducting mafic slab up to the eclogite facies. With Br losses of ~30% and ~60% subducted from basalts and gabbros, respectively, much of the Br that reaches the upper mantle could be introduced by eclogites bearing low Br concentrations (average of ~40 ng/g, Table 3) with Br/Cl ratios averaging $\sim 4.8 \times 10^{-3}$. The Br/Cl ratios measured in Monviso samples are consistent with the ratios reported in OIBs (Kendrick, Jackson, et al., 2015) and from pyroclastic basalts and andesites from Central American volcanic arcs (John et al., 2011).

5.3.4. Iodine

The basalts of the Chenaillet ophiolite have average I concentrations of 76 ng/g, ranging from 65 to 87 ng/g, and ratios of 6.7×10^{-3} I/Cl. Metabasalts from the Monviso ophiolite average 75 ng/g I and range from 72 to 78 ng/g, almost identical to Chenaillet, the modeled protolith (Figure 3). Due to its large ionic size and sensitivity to redox conditions (Kendrick, 2019b), I is highly incompatible and is predicted to be lost early from the slab during dewatering in the forearc. Muramatsu and Wedepohl (1998) documented I losses of 75%–95% from subducting sediments. However, this behavior does not appear to hold for subducted mafic lithologies (Beaudoin et al., 2022), including the Alpine basalts in this study, which appear to retain large portions of their starting I budgets up to high *P-T* metamorphic conditions. The relative immobility of I, indicated by unchanging bulk rock abundances, is supported by the I/Cl ratios in Monviso metabasalts (Figure 4), which average $\sim 10.4 \times 10^{-3}$. The increase in the I/Cl ratio with increasing metamorphic grade is consistent with the more efficient removal of Cl relative to I during subduction.

Retention of I is observed in gabbroic samples from Alpine ophiolites as well. Gabbros from Chenaillet contain, on average, 119 ng/g I and range from 107 to 131 ng/g (Figure 3), with I/Cl ratios averaging 3.3×10^{-3} (Figure 4). This is approximately ~50% more than the blueschist facies metagabbros from the Queyras region ophiolites (average of 63 ng/g I, range of 52–71 ng/g I), suggesting moderate I loss via subduction zone devolatilization. There is a weak positive correlation between I abundances and the abundances of Cl and Br. The correlation is strongest within the Chenaillet samples, where concomitantly high concentrations of Cl, Br, and I may be indicative of more intensive seafloor alteration. The correlations disappear at medium and high grades. The ratios of I/Cl increase slightly between Chenaillet and Queyras (4.1×10^{-3}). However, the loss of I does not continue with an increase in metamorphic grade from blueschist to eclogite facies metagabbros. Samples from Monviso contain 68 ng/g I, on average, and range from 64 to 74 ng/g (Figure 3). The ratio of I/Cl does change however, with the Monviso metagabbros recording I/Cl values averaging 8.2×10^{-3} , a large increase from the Queyras samples, suggesting higher Cl than I mobility during the transition from blueschist to eclogite. Overall, the results of this study suggest that some I is lost from subducting AOC, while some can be retained to high *P-T* conditions and returned to the upper mantle in down-going eclogites.

5.4. Mineralogical Controls on F and Cl Across Metamorphic Grade

Due to its small ionic size and high electronegativity, F is capable of substituting for OH^- in hydrous minerals and has been shown to substitute for O^{2-} in anhydrous phases, such as pyroxene (e.g., Bernini et al., 2013; Beyer

et al., 2012; Urann et al., 2017). In this study, modally abundant F host phases include amphibole, chlorite, epidote, and phengite (Figure 6). In amphiboles, F contents vary from ~ 200 $\mu\text{g/g}$ in ferro-glaucophane from Queyras to $\sim 1,000$ $\mu\text{g/g}$ in actinolite and glaucophane from Chenaillet and Monviso. Similar to amphibole, the concentration of F in epidotes from Chenaillet closely overlaps with those from Monviso, while epidotes from Queyras on average have lower F values. F concentrations in chlorite are broadly consistent across all samples (Figure 6). Phengite is only present in samples from blueschist and eclogite facies. Phengite-hosted F decreases from an average of 2,500 $\mu\text{g/g}$ F in the Queyras sample to 1,000 $\mu\text{g/g}$ F in the Monviso samples. A number of other phases investigated in this work were shown to host F; however, as minor or accessory phases, these minerals do not exert strong controls over the whole rock F budget in the given samples (Figure 6). In sample Q17-H818D01, titanite and apatite each contain $<5\%$ of the whole rock budget, whereas chlorite and phengite contain $\sim 50\%$ and 40% of the F budget. However, an increase in the modal abundance of apatite has the potential to dramatically affect the F budget given its high F content.

Bulk rock compositions show that F concentration is positively correlated with TiO_2 and P_2O_5 content (Figure S1) within the entire sample set. Among the phases analyzed in this study, F concentrations are highest in apatite, ranging from 2.7 to 2.9 wt%. The results of this work demonstrate the ubiquity of F within phases that make up mafic and metamafic assemblages. Additionally, this work shows that while F contents may decrease in some phases with progressive metamorphism (i.e., phengite; Table S4 in Supporting Information S2) among the most modally abundant, F-hosting minerals, the concentration of F remains unchanged from sub-greenschist facies to eclogite facies. To compare, Debret et al. (2016) analyzed F concentrations via SIMS in minerals from similar localities in Chenaillet, Queyras, and Monviso and reported an overall progressive F loss. This is largely due to the high F values (up to $\sim 2,000$ $\mu\text{g/g}$) in amphibole porphyroclasts and coronas from Chenaillet samples used to calculate the bulk rock composition. Actinolite and glaucophane overall had lower concentrations, similar to our observations (Table S4 in Supporting Information S2). We note that Debret et al. (2016) analyzed more samples for in situ measurements than the few analyzed from this study, making direct comparisons between mineral compositions tentative (see Section 5.3.1 above for more discussion on the F budget). This finding supports the conclusion drawn from bulk rock halogen data, demonstrating that F is structurally sited within metamorphic assemblages and is efficiently retained by these phases during prograde metamorphism and devolatilization reactions, resulting in efficient recycling of F to the mantle.

Chlorine is able to substitute into the crystal structure of hydrous minerals via the OH^- site as well; however, it is too large for significant structural incorporation in anhydrous phases. Hydrous minerals that are present in sub-greenschist, blueschist, and eclogite facies assemblages—and predicted to act as Cl hosts—include amphibole, chlorite, and epidote. Using EPMA methods, Cl was not detected at measurable concentrations within chlorites or epidotes from any of the sampling areas investigated (Figure 6). These results are supported by major and trace element compositions, which show no clear correlations to Cl content (Figure S1). At low metamorphic grade, in the Chenaillet ophiolite, actinolite amphiboles contain ~ 300 $\mu\text{g/g}$ Cl on average. In amphiboles, it has been shown that the presence of Fe^{2+} enlarges the octahedral site and enables the larger chloride ion to substitute more easily (Volfinger et al., 1985). While Queyras samples with higher bulk FeO (wt %) contents do tend toward higher Cl abundances, in situ data reveal that the medium- and high-P, Fe-rich amphiboles from the Queyras region and Monviso ophiolite contain very low Cl concentrations (Table S4 in Supporting Information S2), at or below the detection limit of EPMA techniques. Amphibole is an important carrier of Cl during early subduction, as demonstrated by in situ data from Chenaillet. The reduced Cl concentrations of the HP metamorphic amphiboles are consistent with bulk rock trends, which show a reduction in Cl concentrations between Chenaillet and Queyras samples. Amphibole compositions measured by EPMA predict the loss of Cl from subducting AOC relatively early, prior to reaching blueschist facies conditions. Although the Cl concentrations were below detection limits in all medium- and high-P phases analyzed, bulk rock data show that Cl is still present in these samples. At blueschist facies conditions and beyond, Cl is likely distributed at low concentrations among many different minerals or within non-structural sites (e.g., fluid inclusions, grain boundaries, or structural defects). The view that the whole rock Cl budget of subducted ocean crust is not controlled by any particular phase is supported by (a) observations of low Cl concentrations among metamorphic assemblages and (b) the absence of positive correlations between Cl abundances and major and trace element abundances (e.g., K, Ba, Rb) that would be consistent with incorporation in potential host phases (i.e., amphibole or mica).

5.5. Representativeness of Ophiolites in the Western Alps

Alpine ophiolites formed in a slow- to ultraslow-spreading, magma-poor ridge environment in the Alpine Tethys Ocean (e.g., Lagabrielle & Cannat, 1990). Many Alpine ophiolites lack conventional stratigraphy (Tricart & Lemoine, 1991), contributing to the debate regarding the nature and representativeness of these fossil oceanic terrains. The results of this work suggest that, within the context of the halogen system, mafic ophiolitic units from the Western Alps are chemically consistent with other exhumed terrains that formed from the subduction of mature ocean crust. The Chenaillet ophiolite, which has an N-MORB composition (Chalot-Prat et al., 2003) and has been interpreted as a section of obducted ocean crust (Li et al., 2013; Manatschal et al., 2011; Mével et al., 1978), displays bulk halogen concentrations that overlap those measured in AOC drill cores. Chenaillet samples contain between 46 and 164 $\mu\text{g/g}$ F, 11–71 $\mu\text{g/g}$ Cl, 52–112 ng/g Br, and 65–131 ng/g I (Tables 2 and 3). Previous studies have reported halogen contents in AOC basalts and gabbros ranging from approximately 10–300 $\mu\text{g/g}$ F, 10–1,600 $\mu\text{g/g}$ Cl, 40–2,700 ng/g Br, and 0.4–2,400 ng/g I (Figure 4; Beaudoin et al., 2022; Chavrit et al., 2016; Kendrick, 2019a, 2019b).

Only one other study has published bulk F, Cl, Br, and I concentrations of blueschist facies mafic samples. Pagé et al. (2016) investigated a suite of lawsonite blueschists from Turkey and reported halogen concentrations ranging from 222 to 616 $\mu\text{g/g}$ F, 8–22 $\mu\text{g/g}$ Cl, 70–240 ng/g Br, and 130–520 ng/g I (Figure 4). Blueschist facies metagabbros from the Queyras region of the Schistes Lustrés record halogen abundances of 44–125 $\mu\text{g/g}$ F, 9–29 $\mu\text{g/g}$ Cl, 51–89 ng/g Br, and 52–71 ng/g I (Table 3). Although the range in Cl contents is very similar and Br values overlap, F and I abundances are lower in the Alpine mafic blueschists studied here than those from Turkey. Results of this work and others (Beaudoin et al., 2022; Pagé et al., 2016) have found that F and to some extent I are less mobile during devolatilization in mafic rocks than Cl or Br. The relative immobility of metamafic-hosted F and I during subduction supports the interpretation that the disparity in the concentrations of these elements between blueschists from Turkey and those from the Western Alps may be attributed to a difference in protolith concentrations rather than being an indication of fluctuating halogen behaviors within different subduction systems.

Eclogites from the Monviso ophiolite record halogen contents (10–280 $\mu\text{g/g}$ F, 6–9 $\mu\text{g/g}$ Cl, 33–54 ng/g Br, and 64–78 ng/g I; Table 3) that are in close agreement with eclogites from other exhumed oceanic terrains (Figure 4). Beaudoin et al. (2022) reported that eclogites from the Raspas Complex in Ecuador and from Cabo Ortegal in Spain have halogen abundances ranging from 92 to 160 $\mu\text{g/g}$ F, 4–16 $\mu\text{g/g}$ Cl, 17–223 ng/g Br, 35–74 ng/g I and 34–142 $\mu\text{g/g}$ F, 5–34 $\mu\text{g/g}$ Cl, 26–133 ng/g Br, 26–117 ng/g I, respectively. Hughes et al. (2018) conducted a study of halogen contents in HP samples from the Western Alps and found that in metabasalts and metagabbros that equilibrated at eclogite facies conditions, whole rock halogen contents range from <100 to 445 $\mu\text{g/g}$ F, 3–42 $\mu\text{g/g}$ Cl, 4–121 ng/g Br, and 0.3–1.2 ng/g I. The Br and I concentrations in Alpine eclogites from Hughes et al. (2018) extend to very low values, significantly lower than those reported in this work (Figure 4). One possibility for this disparity is the application of different methods to quantify bulk halogen abundances. Hughes et al. (2018) use mineral chemistry (determined by EPMA, time of flight secondary ion mass spectrometry, and neutron irradiation noble gas mass spectrometry) and modal abundances of major mineral constituents to calculate bulk halogen content, with the caveat that not every phase in the samples is analyzed, potentially resulting in undercounting. The methods employed in this study were selected in order to make direct measurements of bulk rock halogen abundances in all phases using the same sample material for F, Cl, Br, and I analyses. The inclusion of all phases could lead to an overestimation in halogen contents as minor retrograde phases, not representative of the peak metamorphic assemblage, could be incorporated during sample preparation. The agreement in halogen concentrations and ratios between this study and others, as well as the positive correlation between Cl and Br values observed in Monviso eclogites from this study, supports the veracity of this dataset and the representativeness of halogen contents in Alpine meta-ophiolites.

6. Summary and Implications for Halogen Geochemical Cycling

Subducting AOC undergoes significant devolatilization during progressive subduction along the path from the trench to the conversion to eclogites prior to depths of arc magma genesis. By investigating a suite of petrologically related ophiolites in the western Alps that represent a prograde metamorphic sequence, this study is able to shed light on the progressive evolution of the halogen budget within subducting AOC. Results of this work show that F is decoupled from the heavy halogens (Cl, Br, and I) and is characterized by immobility within basalts

and gabbros during the fluid-mediated reactions occurring as the rocks transition from sub-greenschist to eclogite facies. The apparent fixity of F based on bulk rock abundances and ratios is supported by in situ data, which show a myriad of modally abundant F-bearing phases that are stable to high P - T conditions. In stark contrast, Cl is highly mobile. Bulk rock abundances and ratios suggest that it is removed from the mafic portion of subducting AOC more efficiently than the other halogens, with extensive devolatilization occurring between the trench and blueschist facies conditions and continuing with the transition to eclogite. EPMA methods only detected Cl-bearing phases at low P - T conditions, confirming that Cl is not incorporated in meaningful quantities within blueschist and eclogitic assemblages. Bromine is removed from subducting AOC less efficiently than Cl because the two elements do show positive correlations in bulk rock data. Over the range of metamorphic conditions studied, the loss of Br via devolatilization appears to occur progressively rather than episodically. No in situ data for Br or I was collected and no potential host phases could be identified based on major or trace element trends. Iodine is mobilized and removed from subducting AOC less efficiently than Cl or Br, with abundances decreasing from low- to -medium-grade before stabilizing and remaining relatively unchanged in the high-grade samples.

Based on the results of this study, significant devolatilization and loss of the initial halogen budget (~60% Cl, ~30% Br, and ~50% I) from gabbros is expected to occur early in subduction, prior to reaching blueschist facies conditions. Much of this released volatile budget is expected to be returned to the surface through the forearc, likely through forearc springs (e.g., Barnes et al., 2018) and along the plate interface or faults coupling this interface to the seafloor (e.g., Mariana forearc; Fryer, 2012). A portion may also be sequestered in the lower crust or sub-continental lithospheric mantle (e.g., Gibson et al., 2020; Segee-Wright et al., 2023). With continued metamorphism and additional halogen losses of ~20% Cl and ~30% Br from metagabbros, AOC undergoes a steady reduction in Cl and Br, while I losses are minimized. The majority of the starting F and approximately 20% of the Cl, 40% of the Br, and 50% of the I survive to eclogite facies. This halogen contribution may be higher if one includes halogens trapped in fluid inclusions (e.g., Herviou et al., 2021). Assuming that the eclogites exposed in the Monviso massif are representative of eclogitic ocean crust that is not exhumed and is instead recycled into the mantle, then these samples demonstrate that AOC may contribute small but chemically significant amounts of F, Cl, Br, and I to the mantle.

Data Availability Statement

Tables S1–S3 in Supporting Information S2 for this manuscript are archived in the Texas Data Repository and are freely available at <https://doi.org/10.18738/T8/K46P5D> (Beaudoin, 2023).

Acknowledgments

The authors wish to thank the members and PIs of the ExTerra Field Institute and Research Endeavor (E-FIRE) group for their support, with special thanks to W. Hoover for assistance with fieldwork, and S. Penniston-Dorland for comments on this manuscript. The authors also thank members and PIs of the “ZIP (Zooming in between plates)” project, particularly for their introductions to the field area. The authors thank J.E. Hoffmann for help setting up the Br-I method at UT-Austin, J. Cullen for help with IC analyses, and G. Segee-Wright for assistance with Br-I data collection. This contribution was improved by helpful and thoughtful comments by two anonymous reviewers and editor W. Behr. This work constituted part of the PhD dissertation of G.M.B. and was funded by the National Science Foundation-Partnerships for International Research and Education (NSF-PIRE) (OIA-1545903) grant. T. John acknowledges funding through Deutsche Forschungsgemeinschaft (DFG, German Research Foundation)—Project-ID 387284271—SFB 1349.

References

- Agard, P. (2021). Subduction of oceanic lithosphere in the Alps: Selective and archetypal from (slow-spreading) oceans. *Earth-Science Reviews*, 214, 103517. <https://doi.org/10.1016/j.earscirev.2021.103517>
- Agard, P., Goffé, B., Touret, J. L. R., & Vidal, O. (2000). Retrograde mineral and fluid evolution in high-pressure metapelites (Schistes lustrés unit, Western Alps). *Contributions to Mineralogy and Petrology*, 140(3), 296–315. <https://doi.org/10.1007/s004100000190>
- Agard, P., Jolivet, L., & Goffé, B. (2001). Tectonometamorphic evolution of the Schistes Lustrés Complex; implications for the exhumation of HP and UHP rocks in the Western Alps. *Bulletin de la Société Géologique de France*, 172(5), 617–636. <https://doi.org/10.2113/172.5.617>
- Aiuppa, A., Baker, D. R., & Webster, J. D. (2009). Halogens in volcanic systems. *Chemical Geology*, 263(1–4), 1–18. <https://doi.org/10.1016/j.chemgeo.2008.10.005>
- Angiboust, S., Langdon, R., Agard, P., Waters, D., & Chopin, C. (2012). Eclogitization of the Monviso ophiolite (W. Alps) and implications on subduction dynamics. *Journal of Metamorphic Geology*, 30(1), 37–61. <https://doi.org/10.1111/j.1525-1314.2011.00951.x>
- Barnes, J. D., Manning, C. E., Scambelluri, M., & Selverstone, J. (2018). The behavior of Halogens during subduction-zone processes. In D. Harlov & L. Aranovich (Eds.), *The role of halogens in terrestrial and extraterrestrial Geochemical processes: Surface, crust, and mantle*, Springer Geochemistry (pp. 545–590). Springer International Publishing.
- Beaudoin, G. (2023). "Data for: "Halogen (F, Cl, Br, and I) devolatilization during prograde subduction: Insights from Western Alps ophiolites"", V1 [Dataset]. *Texas Data Repository*. <https://doi.org/10.18738/T8/K46P5D>
- Beaudoin, G., Barnes, J. D., John, T., Hoffmann, J. E., Chatterjee, R., & Stockli, D. F. (2022). Global halogen cycling of subducting oceanic crust. *Earth and Planetary Science Letters*, 594, 117750. <https://doi.org/10.1016/j.epsl.2022.117750>
- Bernini, D., Wiedenbeck, M., Dolejš, D., & Keppler, H. (2013). Partitioning of halogens between mantle minerals and aqueous fluids: Implications for the fluid flow regime in subduction zones. *Contributions to Mineralogy and Petrology*, 165(1), 117–128. <https://doi.org/10.1007/s00410-012-0799-4>
- Beyer, C., Klemme, S., Wiedenbeck, M., Stracke, A., & Vollmer, C. (2012). Fluorine in nominally fluorine-free mantle minerals: Experimental partitioning of F between olivine, orthopyroxene and silicate melts with implications for magmatic processes. *Earth and Planetary Science Letters*, 337, 1–9. <https://doi.org/10.1016/j.epsl.2012.05.003>
- Blake, M. C., Moore, D. E., & Jayko, A. S. (1995). The role of serpentinite melanges in the unroofing of ultrahigh-pressure metamorphic rocks: An example from the Western Alps in Italy. In R. G. Coleman & X. Wang (Eds.), *Ultrahigh pressure metamorphism* (pp. 182–205). Cambridge University Press.

- Chalot-Prat, F., Ganne, J., & Lombard, A. (2003). No significant element transfer from the oceanic plate to the mantle wedge during subduction and exhumation of the Tethys lithosphere (Western Alps). *Lithos*, 69(3–4), 69–103. [https://doi.org/10.1016/S0024-4937\(03\)00047-1](https://doi.org/10.1016/S0024-4937(03)00047-1)
- Chavrit, D., Burgess, R., Sumino, H., Teagle, D. A. H., Droop, G., Shimizu, A., & Ballentine, C. J. (2016). The contribution of hydrothermally altered ocean crust to the mantle halogen and noble gas cycles. *Geochimica et Cosmochimica Acta*, 183, 106–124. <https://doi.org/10.1016/j.gca.2016.03.014>
- Chopin, C. (1984). Coesite and pure pyrope in high-grade blueschists of the Western Alps: A first record and some consequences. *Contributions to Mineralogy and Petrology*, 86(2), 107–118. <https://doi.org/10.1007/BF00381838>
- Coogan, L. A., Wilson, R. N., Gillis, K. M., & MacLeod, C. J. (2001). Near-solidus evolution of oceanic gabbros: Insights from amphibole geochemistry. *Geochimica et Cosmochimica Acta*, 65(23), 4339–4357. [https://doi.org/10.1016/S0016-7037\(01\)00714-1](https://doi.org/10.1016/S0016-7037(01)00714-1)
- Debret, B., Koga, K. T., Cattani, F., Nicolle, C., Van den Bleeken, G., & Schwartz, S. (2016). Volatile (Li, B, F and Cl) mobility during amphibole breakdown in subduction zones. *Lithos*, 244, 165–181. <https://doi.org/10.1016/j.lithos.2015.12.004>
- Donovan, J. J., Lowers, H. A., & Rusk, B. G. (2011). Improved electron probe microanalysis of trace elements in quartz. *American Mineralogist*, 96(2–3), 274–282. <https://doi.org/10.2138/am.2011.3631>
- Donovan, J. J., Singer, J. W., & Armstrong, J. T. (2016). A new EPMA method for fast trace element analysis in simple matrices. *American Mineralogist*, 101(8), 1839–1853. <https://doi.org/10.2138/am-2016-5628>
- Donovan, J. J., & Tingle, T. N. (1996). An improved mean atomic number background correction for quantitative microanalysis. *Microscopy and Microanalysis*, 2, 1–7. <https://doi.org/10.1017/s1431927696210013>
- Fryer, P. (2012). Serpentinite mud volcanism: Observations, processes, and implications. *Annual Review of Marine Science*, 4(1), 345–373. <https://doi.org/10.1146/annurev-marine-120710-100922>
- Gibson, S. A., Rooks, E. E., Day, J. A., Petrone, C. M., & Leat, P. T. (2020). The role of subcontinental mantle as both “sink” and “source” in deep Earth volatile cycles. *Geochimica et Cosmochimica Acta*, 275, 140–162. <https://doi.org/10.1016/j.gca.2020.02.018>
- Goffé, B., Schwartz, S., Lardeaux, J.-M., & Bousquet, R. (2004). Explanatory notes of the map: Metamorphic structure of the Alps Western and Ligurian Alps. *Mitteilungen der Österreichischen Mineralogischen Gesellschaft*, 125–144.
- Groppo, C., & Castelli, D. (2010). Prograde *P-T* evolution of a Lawsonite Eclogite from the Monviso meta-ophiolite (Western Alps): Dehydration and redox reactions during subduction of oceanic FeTi-oxide gabbro. *Journal of Petrology*, 51(12), 2489–2514. <https://doi.org/10.1093/ptrology/egq065>
- Hauri, E. (2002). SIMS analysis of volatiles in silicate glasses, 2: Isotopes and abundances in Hawaiian melt inclusions. *Chemical Geology*, 183(1–4), 115–141. [https://doi.org/10.1016/S0009-2541\(01\)00374-6](https://doi.org/10.1016/S0009-2541(01)00374-6)
- Herviou, C., Agard, P., Plunder, A., Mendes, K., Verlaquet, A., Deldicque, D., & Cubas, N. (2022). Subducted fragments of the Liguro-Piemont ocean, Western Alps: Spatial correlations and offscraping mechanisms during subduction. *Tectonophysics*, 827, 229267. <https://doi.org/10.1016/j.tecto.2022.229267>
- Herviou, C., Verlaquet, A., Agard, P., Locatelli, M., Raimbourg, H., Lefeuvre, B., & Dubacq, B. (2021). Along-dip variations of subduction fluids: The 30–80 km depth traverse of the Schistes Lustrés complex (Queyras-Monviso, W. Alps). *Lithos*, 394–395, 106168. <https://doi.org/10.1016/j.lithos.2021.106168>
- Hughes, L., Burgess, R., Chavrit, D., Pawley, A., Tartese, R., Droop, G., et al. (2018). Halogen behaviour in subduction zones: Eclogite facies rocks from the Western and Central Alps. *Geochimica et Cosmochimica Acta*, 243, 1–23. <https://doi.org/10.1016/j.gca.2018.09.024>
- Ito, E., Harris, D. M., & Anderson, A. T. (1983). Alteration of oceanic crust and geologic cycling of chlorine and water. *Geochimica et Cosmochimica Acta*, 47(9), 1613–1624. [https://doi.org/10.1016/0016-7037\(83\)90188-6](https://doi.org/10.1016/0016-7037(83)90188-6)
- John, T., Scambelluri, M., Frische, M., Barnes, J. D., & Bach, W. (2011). Dehydration of subducting serpentinite: Implications for halogen mobility in subduction zones and the deep halogen cycle. *Earth and Planetary Science Letters*, 308(1–2), 65–76. <https://doi.org/10.1016/j.epsl.2011.05.038>
- Kendrick, M. A. (2019a). Halogens in altered ocean crust from the East Pacific Rise (ODP/IODP Hole 1256D). *Geochimica et Cosmochimica Acta*, 261, 93–112. <https://doi.org/10.1016/j.gca.2019.06.044>
- Kendrick, M. A. (2019b). Halogens in Atlantis Bank gabbros, SW Indian Ridge: Implications for styles of seafloor alteration. *Earth and Planetary Science Letters*, 514, 96–107. <https://doi.org/10.1016/j.epsl.2019.02.034>
- Kendrick, M. A., Arculus, R. J., Danyushevsky, L. V., Kamenetsky, V. S., Woodhead, J. D., & Honda, M. (2014). Subduction-related halogens (Cl, Br and I) and H₂O in magmatic glasses from Southwest Pacific Backarc Basins. *Earth and Planetary Science Letters*, 400, 165–176. <https://doi.org/10.1016/j.epsl.2014.05.021>
- Kendrick, M. A., Caulfield, J. T., Nguyen, A., Zhao, J., & Blakey, I. (2020). Halogen and trace element analysis of carbonate-veins and Fe-oxyhydroxide by LA-ICPMS: Implications for seafloor alteration, Atlantis Bank, SW Indian Ridge. *Chemical Geology*, 547, 119668. <https://doi.org/10.1016/j.chemgeo.2020.119668>
- Kendrick, M. A., D’Andres, J., Holden, P., & Ireland, T. (2018). Halogens (F, Cl, Br, I) in thirteen USGS, GSJ and NIST international rock and glass reference materials. *Geostandards and Geoanalytical Research*, 42(4), 499–511. <https://doi.org/10.1111/ggr.12229>
- Kendrick, M. A., Danyushevsky, L. V., Falloon, T. J., Woodhead, J. D., Arculus, R. J., & Ireland, T. (2020). SW Pacific arc and backarc lavas and the role of slab-bend serpentinites in the global halogen cycle. *Earth and Planetary Science Letters*, 530, 115921. <https://doi.org/10.1016/j.epsl.2019.115921>
- Kendrick, M. A., Hémond, C., Kamenetsky, V. S., Danyushevsky, L., Devey, C. W., Rodemann, T., et al. (2017). Seawater cycled throughout Earth’s mantle in partially serpentinized lithosphere. *Nature Geoscience*, 10(3), 222–228. <https://doi.org/10.1038/ngeo2902>
- Kendrick, M. A., Honda, M., Pettko, T., Scambelluri, M., Phillips, D., & Giuliani, A. (2013). Subduction zone fluxes of halogens and noble gases in seafloor and forearc serpentinites. *Earth and Planetary Science Letters*, 365, 86–96. <https://doi.org/10.1016/j.epsl.2013.01.006>
- Kendrick, M. A., Honda, M., & Vanko, D. A. (2015). Halogens and noble gases in Mathematician Ridge meta-gabbros, NE Pacific: Implications for oceanic hydrothermal root zones and global volatile cycles. *Contributions to Mineralogy and Petrology*, 170(5–6), 43. <https://doi.org/10.1007/s00410-015-1192-x>
- Kendrick, M. A., Jackson, M. G., Hauri, E. H., & Phillips, D. (2015). The halogen (F, Cl, Br, I) and H₂O systematics of Samoan lavas: Assimilated-seawater, EM2 and high-³He/⁴He components. *Earth and Planetary Science Letters*, 410, 197–209. <https://doi.org/10.1016/j.epsl.2014.11.026>
- Kendrick, M. A., Jackson, M. G., Kent, A. J. R., Hauri, E. H., Wallace, P. J., & Woodhead, J. (2014). Contrasting behaviours of CO₂, S, H₂O and halogens (F, Cl, Br, and I) in enriched-mantle melts from Pitcairn and Society seamounts. *Chemical Geology*, 370, 69–81. <https://doi.org/10.1016/j.chemgeo.2014.01.019>

- Kendrick, M. A., Kamenetsky, V. S., Phillips, D., & Honda, M. (2012). Halogen systematics (Cl, Br, I) in Mid-Ocean Ridge Basalts: A Macquarie Island case study. *Geochimica et Cosmochimica Acta*, *81*, 82–93. <https://doi.org/10.1016/j.gca.2011.12.004>
- Kent, A. J. R., Peate, D. W., Newman, S., Stolper, E. M., & Pearce, J. A. (2002). Chlorine in submarine glasses from the Lau Basin: Seawater contamination and constraints on the composition of slab-derived fluids. *Earth and Planetary Science Letters*, *202*(2), 361–377. [https://doi.org/10.1016/S0012-821X\(02\)00786-0](https://doi.org/10.1016/S0012-821X(02)00786-0)
- Lafay, R., Deschamps, F., Schwartz, S., Guillot, S., Godard, M., Debret, B., & Nicollet, C. (2013). High-pressure serpentinites, a trap-and-release system controlled by metamorphic conditions: Example from the Piedmont zone of the western Alps. *Chemical Geology*, *343*, 38–54. <https://doi.org/10.1016/j.chemgeo.2013.02.008>
- Lagabrielle, Y., & Cannat, M. (1990). Alpine Jurassic ophiolites resemble the modern central Atlantic basement. *Geology*, *18*(4), 319–322. [https://doi.org/10.1130/0091-7613\(1990\)018<0319:ajortm>2.3.co;2](https://doi.org/10.1130/0091-7613(1990)018<0319:ajortm>2.3.co;2)
- le Roux, P. J., Shirey, S. B., Hauri, E. H., Perfit, M. R., & Bender, J. F. (2006). The effects of variable sources, processes and contaminants on the composition of northern EPR MORB (8–10°N and 12–14°N): Evidence from volatiles (H₂O, CO₂, S) and halogens (F, Cl). *Earth and Planetary Science Letters*, *251*(3–4), 209–231. <https://doi.org/10.1016/j.epsl.2006.09.012>
- Li, X.-H., Faure, M., Lin, W., & Manatschal, G. (2013). New isotopic constraints on age and magma genesis of an embryonic oceanic crust: The Chenaillet Ophiolite in the Western Alps. *Lithos*, *160–161*, 283–291. <https://doi.org/10.1016/j.lithos.2012.12.016>
- Manatschal, G., & Müntener, O. (2009). A type sequence across an ancient magma-poor ocean–continent transition: The example of the western Alpine Tethys ophiolites. *Tectonophysics*, *473*(1–2), 4–19. <https://doi.org/10.1016/j.tecto.2008.07.021>
- Manatschal, G., Sauter, D., Karpoff, A. M., Masini, E., Mohn, G., & Lagabrielle, Y. (2011). The Chenaillet Ophiolite in the French/Italian Alps: An ancient analogue for an oceanic core complex? *Lithos*, *124*(3–4), 169–184. <https://doi.org/10.1016/j.lithos.2010.10.017>
- Manning, C. E. (2004). The chemistry of subduction-zone fluids. *Earth and Planetary Science Letters*, *223*(1–2), 1–16. <https://doi.org/10.1016/j.epsl.2004.04.030>
- Mével, C., Caby, R., & Kienast, J.-R. (1978). Amphibolite facies conditions in the oceanic crust: Example of amphibolitized flaser-gabbro and amphibolites from the Chenaillet ophiolite massif (Hautes Alpes, France). *Earth and Planetary Science Letters*, *39*(1), 98–108. [https://doi.org/10.1016/0012-821x\(78\)90146-2](https://doi.org/10.1016/0012-821x(78)90146-2)
- Michel, A., & Villemant, B. (2003). Determination of halogens (F, Cl, Br, I), sulfur and water in seventeen geological reference materials. *Geostandards Newsletter*, *27*(2), 163–171. <https://doi.org/10.1111/j.1751-908X.2003.tb00643.x>
- Muramatsu, Y., Doi, T., Tomaru, H., Fehn, U., Takeuchi, R., & Matsumoto, R. (2007). Halogen concentrations in pore waters and sediments of the Nankai Trough, Japan: Implications for the origin of gas hydrates. *Applied Geochemistry*, *22*(3), 534–556. <https://doi.org/10.1016/j.apgeochem.2006.12.015>
- Muramatsu, Y., & Wedepohl, K. H. (1998). The distribution of iodine in the earth's crust. *Chemical Geology*, *147*(3–4), 201–216. [https://doi.org/10.1016/S0009-2541\(98\)00013-8](https://doi.org/10.1016/S0009-2541(98)00013-8)
- Nadeau, S., Philippot, P., & Pineau, F. (1993). Fluid inclusion and mineral isotopic compositions (H-C-O) in eclogitic rocks as tracers of local fluid migration during high-pressure metamorphism. *Earth and Planetary Science Letters*, *114*(4), 431–448. [https://doi.org/10.1016/0012-821X\(93\)90074-J](https://doi.org/10.1016/0012-821X(93)90074-J)
- Pagé, L., Hattori, K., de Hoog, J. C. M., & Okay, A. I. (2016). Halogen (F, Cl, Br, I) behaviour in subducting slabs: A study of lawsonite blueschists in western Turkey. *Earth and Planetary Science Letters*, *442*, 133–142. <https://doi.org/10.1016/j.epsl.2016.02.054>
- Philippot, P., Agrinier, P., & Scambelluri, M. (1998). Chlorine cycling during subduction of altered oceanic crust. *Earth and Planetary Science Letters*, *161*(1–4), 33–44. [https://doi.org/10.1016/S0012-821X\(98\)00134-4](https://doi.org/10.1016/S0012-821X(98)00134-4)
- Philippot, P., & Selverstone, J. (1991). Trace-element-rich brines in eclogitic veins: Implications for fluid composition and transport during subduction. *Contributions to Mineralogy and Petrology*, *106*(4), 417–430. <https://doi.org/10.1007/BF00321985>
- Schmid, S. M., Pfiffner, O. A., Froitzheim, N., Schönborn, G., & Kissling, E. (1996). Geophysical-geological transect and tectonic evolution of the Swiss-Italian Alps. *Tectonics*, *15*(5), 1036–1064. <https://doi.org/10.1029/96TC00433>
- Schnetger, B., & Muramatsu, Y. (1996). Determination of halogens, with special reference to iodine, in geological and biological samples using pyrohydrolysis for preparation and inductively coupled plasma mass spectrometry and ion chromatography for measurement. *Analyst*, *121*(11), 1627–1631. <https://doi.org/10.1039/AN962101627>
- Schwartz, S., Guillot, S., Reynard, B., Lafay, R., Debret, B., Nicollet, C., et al. (2013). Pressure-temperature estimates of the lizardite/antigorite transition in high pressure serpentinites. *Lithos*, *178*, 197–210. <https://doi.org/10.1016/j.lithos.2012.11.023>
- Segee-Wright, G., Barnes, J. D., Lassiter, J. C., Holmes, D. J., Beaudoin, G. M., Chatterjee, R., et al. (2023). Halogen enrichment in the North American lithospheric mantle from the dehydration of the Farallon plate. *Geochimica et Cosmochimica Acta*, *348*, 187–205. <https://doi.org/10.1016/j.gca.2023.03.014>
- Sekimoto, S., & Ebihara, M. (2017). Accurate determination of chlorine, bromine and iodine in U.S. geological survey geochemical reference materials by radiochemical neutron activation analysis. *Geostandards and Geoanalytical Research*, *41*(2), 213–219. <https://doi.org/10.1111/gr.12145>
- Straub, S. M., & Layne, G. D. (2003). The systematics of chlorine, fluorine, and water in Izu arc front volcanic rocks: Implications for volatile recycling in subduction zones. *Geochimica et Cosmochimica Acta*, *67*(21), 4179–4203. [https://doi.org/10.1016/S0016-7037\(03\)00307-7](https://doi.org/10.1016/S0016-7037(03)00307-7)
- Stronck, N. A., & Haase, K. M. (2004). Chlorine in oceanic intraplate basalts: Constraints on mantle sources and recycling processes. *Geology*, *32*(11), 945–948. <https://doi.org/10.1130/G21027.1>
- Sun, W. D., Binns, R. A., Fan, A. C., Kamenetsky, V. S., Wysoczanski, R., Wei, G. J., et al. (2007). Chlorine in submarine volcanic glasses from the eastern Manus basin. *Geochimica et Cosmochimica Acta*, *71*(6), 1542–1552. <https://doi.org/10.1016/j.gca.2006.12.003>
- Tricart, P., & Lemoine, M. (1991). The Queyras ophiolite West of Monte Viso (Western Alps): Indicator of a peculiar ocean floor in the mesozoic tethys. *Journal of Geodynamics*, *13*(2–4), 163–181. [https://doi.org/10.1016/0264-3707\(91\)90037-F](https://doi.org/10.1016/0264-3707(91)90037-F)
- Tricart, P., & Schwartz, S. (2006). A north-south section across the Queyras Schistes lustrés (Piedmont zone, Western Alps): Syn-collision refolding of a subduction wedge. *Eclogae Geologicae Helveticae*, *99*(3), 429–442. <https://doi.org/10.1007/s00015-006-1197-6>
- Urrant, B. M., Roux, V. L., Hammond, K., Marschall, H. R., Lee, C.-T. A., & Monteleone, B. D. (2017). Fluorine and chlorine in mantle minerals and the halogen budget of the Earth's mantle. *Contributions to Mineralogy and Petrology*, *172*(7), 51. <https://doi.org/10.1007/s00410-017-1368-7>
- Urrant, B. M., Roux, V. L., John, T., Beaudoin, G. M., & Barnes, J. D. (2020). The distribution and abundance of halogens in eclogites: An in situ SIMS perspective of the Raspas Complex (Ecuador). *American Mineralogist*, *105*(3), 307–318. <https://doi.org/10.2138/am-2020-6994>
- Volfinger, M., Robert, J.-L., Vielzeuf, D., & Neiva, A. M. R. (1985). Structural control of the chlorine content of OH-bearing silicates (micas and amphiboles). *Geochimica et Cosmochimica Acta*, *49*(1), 37–48. [https://doi.org/10.1016/0016-7037\(85\)90189-9](https://doi.org/10.1016/0016-7037(85)90189-9)

- Whitney, D. L., & Evans, B. W. (2010). Abbreviations for names of rock-forming minerals. *American Mineralogist*, 95(1), 185–187. <https://doi.org/10.2138/am.2010.3371>
- Zhang, C., Wang, L.-X., Marks, M. A. W., France, L., & Koepke, J. (2017). Volatiles (CO₂, S, F, Cl, Br) in the dike-gabbro transition zone at IODP Hole 1256D: Magmatic imprint versus hydrothermal influence at fast-spreading mid-ocean ridge. *Chemical Geology*, 459, 43–60. <https://doi.org/10.1016/j.chemgeo.2017.04.002>